A study on modeling and compensation of the rate-dependent hysteresis of a piezo electric actuator based on soft computing

September 2016

Liu Dongbo

Graduate School of Science and Engineering
Yamaguchi University

Abstract

This dissertation summarizes the results of the studies on modeling and compensation of the rate-dependent hysteresis of a piezo-electric actuator, based on the soft computing staffs.

Smart materials are the materials which respond to the exogenous physical stimuli. They are commonly found in many engineering applications as a part of smart systems. Piezo electric material inflates in the direction of electrical field when voltage is applied. Piezo electric actuator is a prime application of the piezo electric material which has the distinctive advantages of solid state actuation, compact size, high precision, high stiffness and quick responses. It is widely used in engineering applications like vibration control, machine tool control, high-precision positioning control and many others.

However, it is known that piezo electric actuator suffers hysteresis which might lead to considerable deterioration of positioning accuracy without appropriate compensation. It is also recognized by practitioners and researchers in the field that real-world piezo actuators might exhibit drastic change in their hysteretic behavior when the rate or the frequency of their driving signal varies. This phenomenon is referred to as the rate-dependent hysteresis. Extensive research efforts have been devoted to both mathematical hysteresis modeling and the compensation of hysteresis.

Many mathematical models have been proposed to capture the nonlinear behavior of hysteresis. Examples include the Preisach model, Play / Stop models, Bouc-Wen model, Maxwell slip model and Duhem model. However, it is not a good choice to use Preisach or Play / Stop models to capture rate dependent hysteresis because vast amount of calculation is inevitable to prepare the database of distribution functions to cover the entire range of driving conditions. In order to reduce the amount of calculation necessary to capture the rate-dependent behavior of the piezo actuator, use of models which contain few parameters and the repeat the parameter identification would be a natural thought. Thus I have formulated the radial basis function neural network model and trained it to exhibit a rate-dependent input/output hysteretic behavior. I also have used the classical Bouc-Wen model to do the same thing. These two choices would finally result in the same problem to find the set of parameters which best fits the input/output

data used for training. I have proposed the membrane structure genetic algorithm as a solver of the included parameter identification problem. Several classical global search algorithms have been applied to both two models in order to discuss how only the structure of the model affects the fitting result.

Enormous amount of studied have been reported about the hysteresis compensation of piezo actuator. The study include the feedforward approach which mainly uses inverse hysteretic mapping as a compensator and the feedback control approach. This study proposes the internal model control with two radial basis function networks: one used as the internal model of the piezo actuator and the other used as the feedback controller of the system. Experimental results with time varying frequency pure sinusoidal position reference signal were given to evaluate the performance of the proposed control system.

This dissertation is divided into 5 chapters.

Chapter 1 introduces the previous research about hysteresis modeling and compensation, and explains the background of the works and overview of the dissertation.

Chapter 2 dictates soft computing tools such as radial basis function neural network, particle swarm optimization, genetic algorithm and membrane computing and introduces rate-dependent hysteresis behavior of piezo electric actuator. Furthermore, In order to improve the research of hysteresis modeling and compensation of piezo electric actuator, a description of membrane structure genetic algorithm which is hereafter abbreviated as MSGA is presented in this chapter.

Chapter 3 describes the modeling of the rate-dependent hysteresis of piezo electric actuator. The Bouc-Wen model and the RBF neural network model for hysteresis modeling of our piezo electric actuator are conducted, the parameters optimization based on soft computing is applied for the hysteresis models in this chapter too. In order to find the influence of the modeling performance by the models and optimization methods, the comparison of the two models based on tree different methods is given to analyze the results.

Chapter 4 introduces the control strategy for the compensation for hysteresis of piezo electric actuator. Based on the last chapter, an adaptive internal model control design with double RBF neural networks for compensation of rate-dependent hysteresis of a piezo actuator is proposed. Internal

model control design basically requires precise model of a controlled-process, one RBF neural network is trained with the help of particle swarm optimization algorithm to perform as the internal model of a piezo electric actuator with rate-dependent hysteresis which is a necessary element to synthesize internal model control, while the other RBF neural network is given the role of a controller of the feedback control. The control results and analysis of the experiments are shown in this chapter too.

Finally, conclusion has been drawn in Chapter 5.

要旨

本稿は，ソフトコンピューティングの手法を用いたピエゾアクチュエータの速度依存ヒステリシス特性を表すモデルの構築と，その補償制御系の構成に関する著者の研究結果をまとめたものである。

スマート材料は，外部刺激に何らかの反応を示す材料のことで，機械システムにおけるセンサやアクチュエータ，ON/OFF の論理素子的挙動が求められる応用など様々な場面で多く活用されている．スマート材料の一つであるピエゾ素子は，電圧が加えられると電界の方向に伸展する特徴を持っている．ピエゾアクチュエータは，ピエゾ素子の優れた応用製品の一つであり，サイズが小さいこと，高精度の変位制御が可能であること，高剛性を有すること，速応性が高いことなど，多くの好ましい特徴を有しており，制振制御，工作機械，電子顕微鏡の高精度位置決め制御など数多くの場面で応用されている．

しかしながら，ピエゾアクチュエータは入出力特性にヒステリシスを示すこと，および駆動の速度／周波数を変更するとヒステリシスの特徴が変化することが良く知られており，後者は特に速度依存ヒステリシス現象と呼ばれている．ピエゾアクチュエータの高精度位置決め制御の応用においては，これらのヒステリシスに適切な補償を行わないと位置決め精度が非常に悪化することから，ピエゾアクチュエータのヒステリシス補償に関しては数多くの研究がなされている．それらは，ヒステリシス特性の数学モデルの構築に関する提案を主眼とするものと，ヒステリシス補償要素の設計方法の提案に関するものに大別される．ヒステリシス特性のモデル化に関しては，Preisach モデルをはじめとして，Play/Stop モデル，Bouc-Wen モデル，Maxwell slip モデルや Duhem モデルなど様々なモデルが提案されている．しかし，Preisach モデルや Play / Stop モデルのように分布関数の同定が必要なモデルについては，分布関数の同定に大量の計算が必要になるものの，それにより得られるヒステリシス特性は，速度依存の特性変化を示さないため，速度依存ヒステリシスへの適用に際しては駆動条件に応じた再同定が必要となり得策ではない．そこで本研究では，ヒステリシス非線形性を放射基底関数 (RBF) を利用した RBF ネットワークに学習獲得させることで数学的構造の変更を必要としないヒステリシス特性のモデル化法と，決定すべきパラメータ数が少ない Bouc-Wen モデルの構造に複数の数値最適化手法を組み合わせて速度依存ヒステリシスモデルを同定する 2 つの方法を検討した．最終的にはどちらも実験で得られた入出力データに対する最良の当てはめを提供するパラメータ探索の問題になる．本研究では，Membrane computing と遺伝的アルゴリズムを組み合わせた MSGA による大域的パラメータ探索法を提案し用いるが，

他の既知の最適化手法も比較検討のために利用して，モデリングにおける数値最適化手法の得失の評価を併せて行う．

一方，ヒステリシス特性の補償に関しても数多くの先行研究が存在しているが，それらはフィードフォワード制御によるものと，センサを利用してフィードバック制御を構築するものの２つに大別することができる．本研究では，Morari らによる内部モデル制御をヒステリシス補償制御系に利用する方法を検討した．徐々に周波数が変化する正弦波信号を目標値とした実験によりその有効性を評価する．本稿は５章からなる．まず第１章では，ピエゾアクチュエータのヒステリシス特性のモデリングとヒステリシス補償に関する先行研究を整理した上で，本研究の狙いと目的を述べる．第２章では，RBF ネットワーク，粒子群最適化 (Particle Swarm Optimization : PSO) 法，遺伝的アルゴリズム (Genetic Algorithm : GA) および membrane computing 法など，ヒステリシス特性のモデリングと補償で利用するツールや手法をまとめる．また，著者の独自の提案となる，membrane computing の数学的構造に遺伝的アルゴリズムを組み込んだ MSGA (Membrane Structure Genetic Algorithm) 法について説明を加える．

第３章では，ピエゾアクチュエータの速度依存ヒステリシス特性のモデリングについて論じる．上述のとおり，特定の数式構造に依存しないモデルとして RBF ネットワークを利用したモデルを提示するとともに，数式が表現する構造に依存したモデルとしてパラメータ数の少ない Bouc-Wen モデルを取り上げ，著者が評価実験で利用したピエゾアクチュエータのヒステリシス特性のモデリング性能を評価した．その際，モデルパラメータの最適化手法の差異がデータ当てはめ精度に与える影響を排除するため，両方のモデルに等しい最適化手法を適用し，モデル構造に絞ったあてはめ精度の議論が可能となるようにした．結果は，実験で測定したデータに対するあてはめの良さで優劣が論じられる．

第４章では，前章までの議論に基づき，ピエゾアクチュエータの速度依存ヒステリシス特性を補償する制御系の構成について示す．提案する制御系は内部モデル制御の構造を有している．内部モデルとして前段のモデリングに関する検討で得られた RBF ネットワークによるモデルを用いるとともに，駆動信号の周波数変化による制御対象のピエゾアクチュエータのヒステリシス特性変化を補償するためコントローラにも RBF ネットワークを利用するダブルネットワーク型の構造を採用した．提案した制御系の性能を，実験により評価する．

最後に５章で，本研究により得られた結果をまとめるとともに，今後の研究の展開に言及する．

Contents

Chapter 1

Introduction

1.1 Background

Smart materials integrate the function of sensing, actuation, logic and control to respond adaptively to the changes of their environment in a useful and usually repetitive manner. They are commonly found in many engineering applications usually as a part of smart systems. Piezo electric material shrinks in the direction of electrical field when driving voltage is applied. A variety of existing engineering materials can be utilized as a sensor as well as actuator if being properly designed. Piezo electric actuator is a prime application of the piezo electric material which has the distinctive advantages of solid state actuation, compact size, high precession, high stiffness and quick responses. It is widely used in engineering applications like vibration control[1, 2], machine tool control[3], high-precision positioning control[4, 5] and many others[6, 7].

However, it is also known that piezo electric actuator suffers hysteresis which might lead to considerable deterioration of positioning accuracy without appropriate compensation[8]. It is commonly recognized by practitioners and researchers in the field that real-world piezo actuators might exhibit drastic change in their hysteretic behavior when the rate or the frequency of their driving signal varies. This phenomenon is called the rate-dependent hysteresis. Compensation of rate-dependent hysteresis is a challenging problem and attracts interest of researchers. Extensive research efforts have been

devoted to the hysteresis compensation of piezo actuators which can generally be divided to two major problems. One is the modeling of hysteretic behavior and the other is the controller synthesis.

In order to capture the property of hysteresis for piezo electric actuator, vast amounts of studies have been conducted by the researchers in this field which use mathematical models like Preisach model[11–14], Bouc-Wen model[15–18], Maxwell slip model[19–22] and Duhem model[23–26]. Following the pioneering research on the mathematical modeling of hysteresis by Franz Preisach in 1935[9], Mayergoyz has given necessary and sufficient conditions for the representation of hysteresis nonlinearity with his scalar Preisach model[10]. Yu et al. proposed dynamic Preisach modeling of hysteresis for the piezo electric actuator[37]. Ueda et al. proposed an ALC model for hysteresis where the states of magnetization of the discretized Preisach plane constitute the input signal sequence of ALC[38]. Preisach model has also been successfully applied to many engineering problems. Bouc-Wen model is proposed by Bouc initially in 1971[39] and extended by Wen in 1976[40]. Bouc-Wen model is capable of capturing the property of a wide class of hysteretic systems and it has been extensively used in many engineering applications such as magnetohydrodynamical dampers[41], base isolation devices[42], and mechanical systems[43]. Lee et al. used a nonlinear differential equation based on Bouc-Wen model to express hysteresis for precise tracking control of a peizo actuator[44]. Maxwell slip model was used to express hysteresis by Yeh et al and it was reported that this model was successfully adapted to capture both symmetric and asymmetric hysteretic loops[45]. Tri et al. used Maxwell slip model to describe hysteretic behavior of the pneumatic artificial muscle to control its contraction[46], but the assumption on the rising curve of hysteresis which yields the actuator to start its motion from a relaxed state is difficult to be satisfied for some applications. Wang et al. presented hysteresis compensation in giant magnetostrictive actuators using Duhem model[47].

However, because of their definitive mathematical structures, these models require parameter identifications before they are actually used in the model based controller design. Some require considerably large amount of data and calculation in order to determine all the parameters included in the model to capture a single hysteretic motion of the system, and it might become void if the target device exhibits rate/frequency-dependent hysteresis. If the model is not sufficiently accurate, the resulting hysteresis compensation performance can be poor and/or the control system might be very conservative.

A tremendous amount of results on the compensation of hysteresis nonlinearity have been reported in literature which is basically classified to feedforward approach[27–31] and feedback approach[31–36]. Rosenbaum et al. proposed a feedforward control using inverse Preisach model for accurate control of electromagnetic actuators[48]. Another feedforward compensation control system was utilized for piezo actuator system based on an exact inversion of the model under the condition that the distances between the thresholds do not increase in time[49]. Rakotondrabe proposed an inverse multiplicative structure of a compensator scheme for the hysteresis nonlinearity which was expressed by Bouc-Wen model[50]. An optimal PID control was utilized to improve tracking performance of a piezoelectric positioner at low frequencies by Shieh et al.[51]. Lu et al. decentralized sliding mode control for a steel frame micro-manipulator[52]. Lin presented neural network adaptive control and repetitive control for precise motion control applications[53]. A state feedback control approach was applied to the piezoelectric actuator for diamond turning machines by Okazaki[54]. Recently, Hata et al. have designed a parametrized feedforward controller using Preisach model for the compensation of rate-dependent hysteresis[55]. The inverse distribution function is generated off-line by an interpolation of two inverse distribution functions identified at two extremal driving frequencies to avoid elaborative work of determining a large number of inverse distribution functions for many different operating conditions, and their controller exhibits acceptable performance for a wide range of frequencies but the positioning accuracy and tracking performance of the control system will possibly be deteriorated if the response characteristics deviate largely due to resonance because it will lead to increased inaccuracy of the models used in control input synthesis.

In order to solve the complex problems of traditional research technique, the idea and use of neural network and bio inspired algorithms give the new idea and direction to solve the problems in control field. The bio inspired algorithm such like genetic algorithm (GA), particle swarm optimization (PSO), artificial fish-swarm optimization and membrane computing promote the improvement and development of the control research. Membrane computing proposed by Ghoerghe Paun is a new computing method inspired from the structure and function of living cells model which is also called the P system[68].

Many researches about bio inspired algorithms can be found in the literature. The genetic algorithm was proposed for optimization of PID controller on the electro-hydraulic servo control System[75]. A fuzzy logic controller with PSO was proposed for 2 DOF robot trajectory control[76]. The

membrane computing are successfully applied to many engineering problems. The membrane systems were applied for the knee joint injury and repair model[77]. A stochastic membrane system was also applied for metapopulations modeling[78]. In order to improve the research of hysteresis modeling and compensation based on membrane computing, inspired from membrane computing and genetic algorithm, a membrane structure genetic algorithm which is hereafter abbreviated as MSGA is utilized to improve the performance of this research.

Bouc-Wen model is a mathematical model for capturing the property of a wide class of hysteresis. The hysteresis modeling of Bouc-Wen model with membrane structure genetic algorithm proposed first in this dissertation. Neural network can be a powerful system identification tool, which has good ability in approximating nonlinear mappings, and the model identification performed by neural network is applied for piezo electric actuators in this research. Furthermore, because RBF neural network which is abbreviated hereafter as RBFNN has better ability of approximating nonlinear mappings, ease of generalization, fast convergence of training process and simplicity of architecture, then an RBFNN hysteresis modeling with PSO is proposed for piezo electric actuator. All the comparison between two models based different methods is given at last.

The intrinsic difficulty of model based control system for rate-dependent hysteresis is coming from the fact that mathematical structure of the model is fixed. This observation leads to the idea to incorporate numerical mapping staffs into the control system to capture rate-dependent hysteresis and utilize it in the controller design. An adaptive feedback control system design for compensation of rate-dependent hysteresis of a piezo actuator is presented in the dissertation. In this research, the proposed control system design is based on the structure of internal model control (IMC) originally proposed by Morari and Zafirious in 1989[79]. The IMC basically requires precise model of a controlled-process. This control strategy adopts two radial basis function neural networks to construct a high precision positioning control system of a piezo electric actuator which exhibits rate-dependent hysteresis.

The experimental results indicate that the proposed control strategies have adequate performance on the compensation of hysteresis to guarantee high precision in positioning control for the piezo electric actuator.

1.2 Overview

This dissertation summarizes the results and the works on modeling and compensation of the rate-dependent hysteresis a piezo electric actuator based on soft computing, where RBF neural networks and bio inspired algorithms are extensively used as a key technical tool. The dissertation will be divided to five chapters.

Chapter 1 introduces the previous research about hysteresis modeling and compensation, and explains the background of the works and overview of the dissertation.

Chapter 2 dictates the preliminaries. The rate-dependent hysteresis of piezo electric actuator are described, soft computing tools such as radial basis function neural network, particle swarm optimization, genetic algorithm and membrane computing are introduced. Membrane computing proposed by Gheorghe Paun is a branch of natural computing which investigates computing models abstracted from the structure, the functioning of living cells. Furthermore, In order to improve the research of classical methods of hysteresis modeling and compensation, a membrane structure genetic algorithm proposed for fast global optimization is also described in this chapter.

Chapter 3 describes modeling of the rate-dependent hysteresis of piezo electric actuator. The Bouc-Wen model and the RBF neural network model for hysteresis modeling of our piezo electric actuator are conducted, the parameters optimization based on soft computing is applied for the hysteresis models in this chapter too. In order to find the influence of the modeling performance by the models and optimization methods, the comparison of the two models based on tree different methods is given in this chapter too.

Chapter 4 introduces the control strategy for compensation for the rate-dependent hysteresis of a piezo electric actuator. This chapter describes an adaptive feedback Internal model control system design for compensation of rate-dependent hysteresis of a piezo actuator. TBased on the last chapter, an adaptive internal model control design with double RBF neural networks for compensation of rate-dependent hysteresis of a piezo actuator is proposed. Internal model control design basically requires precise model of a controlled-process, one RBF neural network is trained with the help of particle swarm optimization algorithm to perform as the internal model of a piezo electric actuator with rate-dependent hysteresis which is a necessary element to syn-

thesize internal model control, while the other RBF neural network is given the role of a controller of the feedback control system. The control experimental results and analysis based on the proposed control system have also been given in this chapter

Finally, conclusion has been drawn in Chapter 5.

Chapter 2

Preliminaries

2.1 Phenomenological Models of Hysteresis

2.1.1 Preisach Model

The Preisach model proposed by Franz Preisach is the most popular operator-based model in order to capture the property of hysteresis for piezo electric actuator. Generally, Preisach model can be expressed by a double integrator equation as defined by

$$x(t) = \iint_{\alpha \geq \beta} \mu(\alpha, \beta) \gamma_{\alpha\beta}[u(t)] d\alpha d\beta, \tag{2.1}$$

where $x(t)$ is the displacement output of the actuator, $\mu(\alpha, \beta)$ is a distribution function , the hysteresis operator $\gamma_{\alpha\beta}[u(t)]$ has an output value of -1 or $+1$ upon the polarized direction of input $u(t)$ corresponding to up and down switching values of the operator as shown in Fig.2.1. The distribution function $\mu(\alpha, \beta)$ selected by experience and experiments determines the shape of the hysteresis curve. The triangular domain of integration of Eq.(2.1) in (α, β) plane is called the Preisach plane as shown in Fig.2.2.

Considering the positive part T^+ and the negative part T^- in the hys-

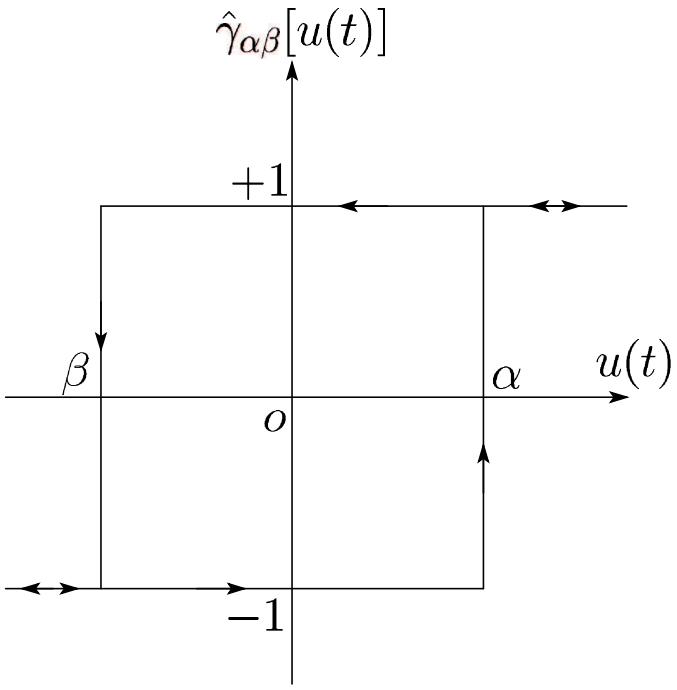

Figure 2.1 The hysteresis operator $\gamma_{\alpha\beta}$

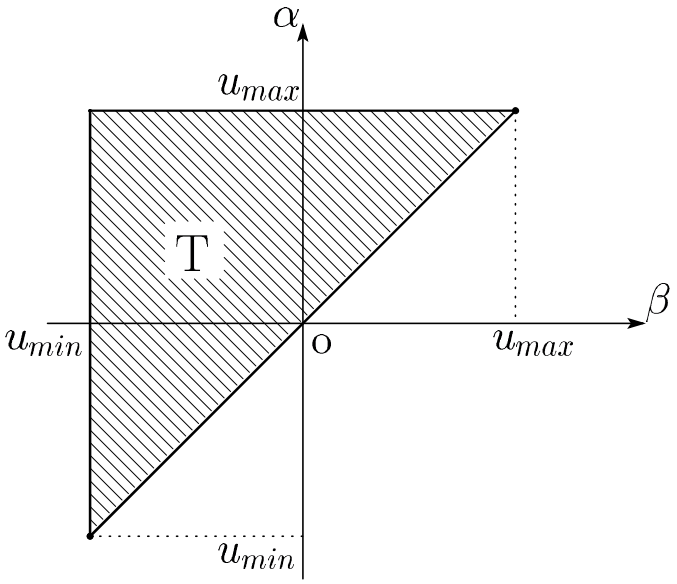

Figure 2.2 Planet of Preisach model

teresis operator, Eq.(2.1) can be rewritten by

$$f(u) = \iint_{T^+} \mu(\alpha,\beta)d\alpha d\beta - \iint_{T^-} \mu(\alpha,\beta)d\alpha d\beta \tag{2.2}$$

$$= \iint_{T^+} \mu(\alpha,\beta)d\alpha d\beta - \iint_{T^m - T^+} \mu(\alpha,\beta)d\alpha d\beta \tag{2.3}$$

$$= 2\iint_{T^+} \mu(\alpha,\beta)d\alpha d\beta - \iint_{T^m} \mu(\alpha,\beta)d\alpha d\beta, \tag{2.4}$$

where T^m is when the whole entire area of T become positive. Preisach model is used in the discretized form in the practical implementation. The Preisach plane and the corresponding distribution function should be discretized accordingly. Let the interval $[u_{min}, u_{max}]$ be discretized into n small intervals $[u_{n-1}, u_n]$, $(n = 1, 2, \cdots, N)$. The discretized distribution function can be calculated by

$$\mu'(i,j) = \int_{u_{j-1}}^{u_j} \int_{u_{i-1}}^{u_i} \mu(\alpha, \beta) d\alpha d\beta, \tag{2.5}$$

which corresponds to (i,j)-th cell of a discretized Preisach plane. The discrete version of Eq.(2.4) is given by

$$f(u) = 2 \sum_{i=1}^{N} \sum_{j=1}^{i} \mu'(i,j) T'(i,j) - \sum_{i=1}^{N} \sum_{j=1}^{i} \mu'(i,j), \tag{2.6}$$

where $T'(i,j)$ represents how (i,j)-th cell is magnetized. $T'(i,j)$ takes the value 1 when the cell is positively magnetized, otherwise it takes the value 0[55, 56].

As mentioned in chapter 1, the Preisach model is widely used in hysteresis modeling. A modified Preisach model is proposed for an integrated piezo-driven cantilever beam under quasi-static condition[57]. In a type of hybrid model, the tabulated Everette function is used in terms of the Preisach model to reduce the number of data points required in the classical Preisach model[58]. A PID optimal control using Preisach model is designed for a shape memory alloy actuator[59]. Although the Preisach model is widely used for hysteresis characterization, it also has some disadvantages. For instance, it requires large quantity of databases and experiments to identify the distribution function which influences the accuracy, it is also inconvenient when using it for real-time online systems, and it has difficulties in research of rate-dependent hysteresis because of rate-independent model.

2.1.2 Bouc-Wen Model

Bouc-Wen model introduced by Bouc and extended by Wen is another mathematical model for capturing the property of a wide class of hysteresis. Bouc-Wen model has been extensively used in the current literature to describe the behavior of components and devices with hysteresis. It is frequently used in the areas of civil and mechanical engineering.

Generally, the Bouc-Wen model can be expressed in the form of the nonlinear differential equation defined by

$$\dot{z} = \alpha\dot{u} - \beta|\dot{u}||z|^{n-1}z - \gamma\dot{u}|z|^{n}, \tag{2.7}$$

where α, β, γ and n are the parameters of the model which govern the shape and the magnitude of hysteresis, z is a state variable, and $\dot{u}$ is the derivative of the input. Figs.2.3,2.4,2.5,2.6 show how different parameters would affect the shape of the resulting hysteretic behavior of the Bouc-Wen model. It can be found from the figures that α controls the restoring force amplitude of Bouc-Wen model, β and γ control the shape of the trajectory, and n controls the smoothness of the transition from elastic to plastic response.

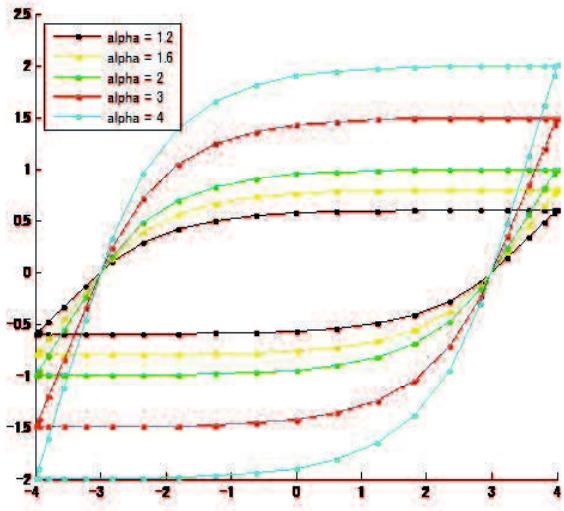

Figure 2.3 How α affects the response of Bouc-Wen model($\beta = 1$, $\gamma = 1$, $n = 1$)

The Bouc-Wen model is capable of capturing input/output behavior for a wide class of hysteretic systems, and it can also be used for piezo actuators. A fuzzy-based PD controller is synthesized for a piezo actuator[60]. A backstepping nonlinear control using identified Bouc-Wen model is proposed for a piezo actuator to improve the performance of nonlinear system[61].

However, Bouc-Wen model also has some disadvantages. Although Bouc-Wen model just requires one auxiliary nonlinear differential equation which features computational simplicity, the rate-independent property and symmetric structure of Bouc-Wen model will restrict the range of application

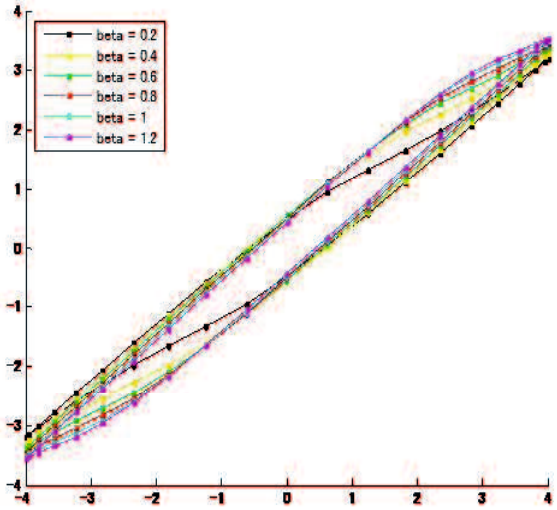

Figure 2.4 How β affects the response of Bouc-Wen model($\alpha = 1$, $\gamma = 1$, $n = 1$)

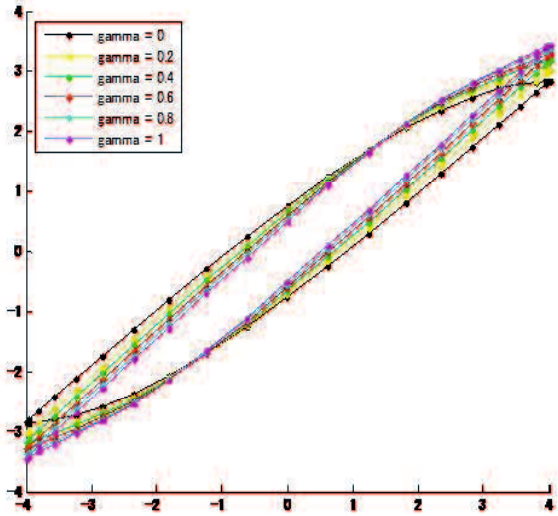

Figure 2.5 How γ affects the response of Bouc-Wen model($\alpha = 1$, $\beta = 1$, $n = 1$)

of Bouc-Wen model. Some researchers modified the structure of Bouc-Wen model in order to achieve hysteresis modeling accurately. Using system iden-

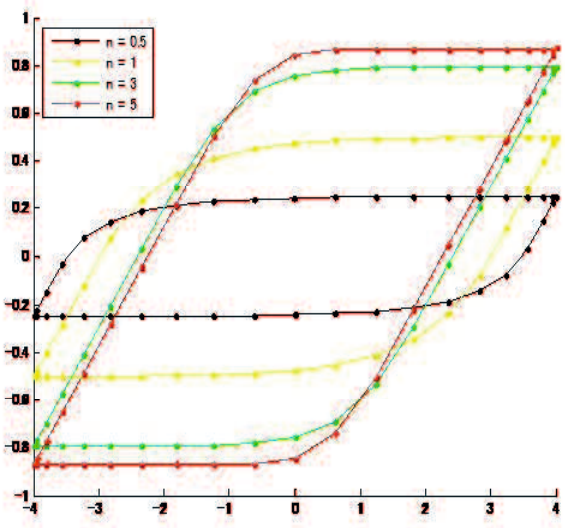

Figure 2.6 How n affects the response of Bouc-Wen model($\alpha = 1$, $\beta = 1$, $\gamma = 1$)

tification techniques to perform parameter identification of Bouc-Wen model is one way possible improvement of the Bouc-Wen model.

2.2 Rate-dependent Hysteresis of Piezo Electric Actuator

2.2.1 Piezo Electric Actuator

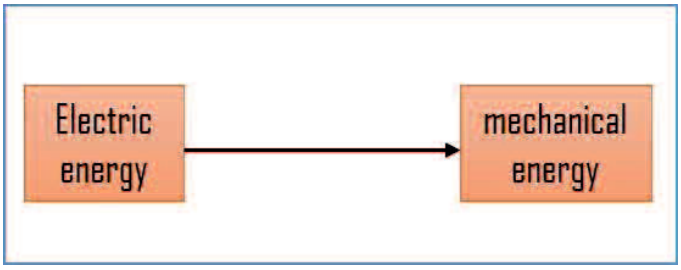

Figure 2.7 Principle of piezo electric actuator

Piezo electric actuator is a prime application of the piezo electric material which has the distinctive advantages of solid state actuation, compact size, high precision, high stiffness and quick responses.

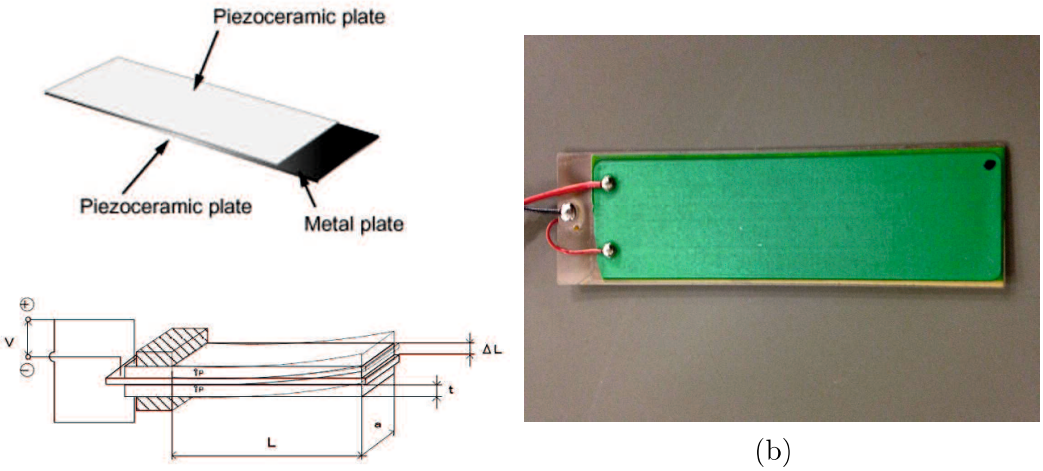

(a) (b)

Figure 2.8 Piezo electric actuator

It converts an electrical driving signal into physical displacement as displayed in Fig.2.7. In the case where active layer is piezoelectric, deformation in that layer may be induced by the application of an electric field. This deformation induces a bending displacement of the cantilever. There are

two types of bending actuators, unimorph and bimorph. The unimorph or monomorph type piezo electric actuator is a cantilever that consists of one active layer and one inactive layer. The bimorph type piezo electric actuator has two layers of piezo electric actuator.

Fig.2.8 shows the bi-morph type piezo electric actuator (PZBA-00030 manufactured by FDK Corporation) used in the experiments in this dissertation.

2.2.2 Experimental setup

The bi-morph type piezo electric actuator and a non-contacting type displacement sensor used in this research is shown in Fig.2.9. Physical parameters of the actuator are summarized in Table 2.1.

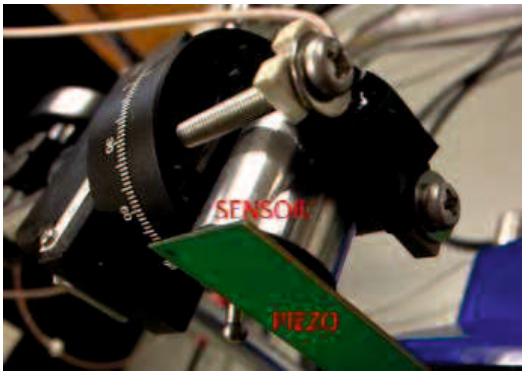

Figure 2.9 Apparatus of experiment

Fig.2.10 shows the experimental setup. The input signals are generated with a D/A interface installed in the PC which is amplified by the piezo driver (As-904, NF) to drive the piezo electric actuator. The system is controlled in real time by a PC in which ART-Linux[62] is installed as a real time operating system. Displacement of the actuator is measured with a non-contacting type displacement sensor (M-2213, MESS-TEK Corporation) with dynamic range of $\pm 1000[\mu\mathrm{m}]$ and a positioning resolution of 20[nm]. The sensor output is provided in the form of an analogue voltage which is read by an A/D interface, 1[ms] sampling interval is used in all experiments disclosed in this dissertation.

We have also used an alternate laser displacement sensor (LK-G30 Keyence)

Table 2.1 The physical parameters of piezo electric actuator PZBA-00030

Width[mm]	20
Length[mm]	65
Thickness[mm]	0.5
Displacement[mm/70v]	0.6
Natural Frequency[HZ]	103

Table 2.2 Details of Keyence laser sensor LK-G30

Reference distance[mm]	30
Measuring range[mm]	±5
Mass[g]	280
Resolution of laser[mm/V]	0.5

to see how measurement accuracy will affect precision of the modeling and control of piezo electric actuator. Details of Keyence laser sensor are summarized in Table 2.2.

2.2.3 Rate-dependent Hysteresis

Hysteresis is the time-based dependence of a system output on the present and the past inputs. The dependence arises because the history affects the value of an internal state. In order to predict its future outputs, either its internal state or its past input must be known[63]. The phenomenon can be observed in the form of the hysteresis loop in the input/output plane as shown in Fig.2.11. Presence of hysteresis introduces nonlinearities between the input and the output. It causes positioning errors which significantly hinder the operating speed and precision of the piezo electric actuator.

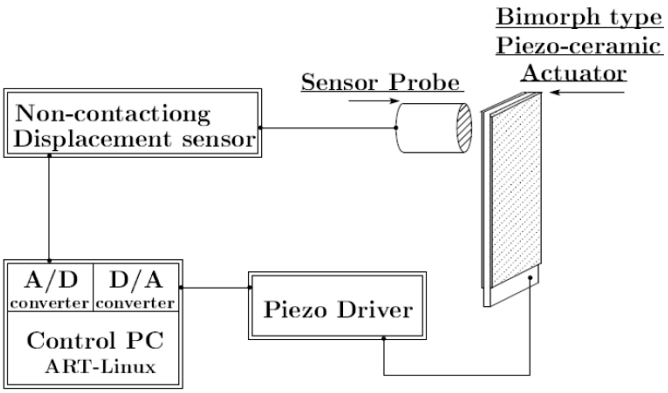

Figure 2.10 Schematic diagram of the experiment

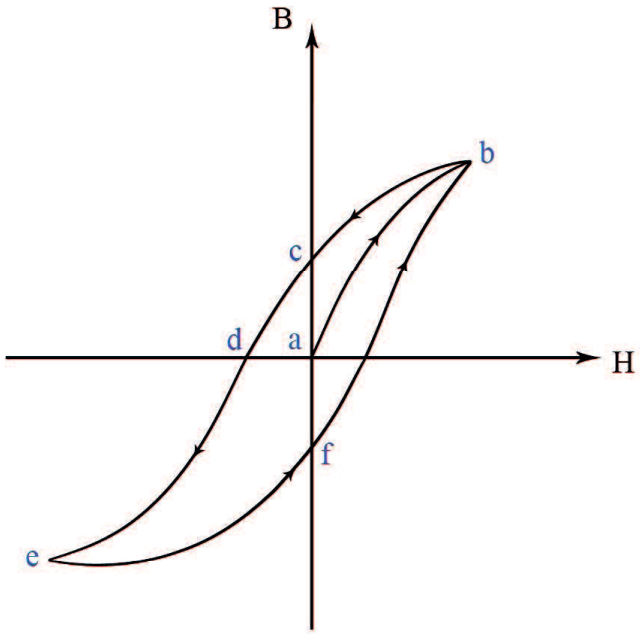

Figure 2.11 An example of the hysteresis

However, the piezo electric actuator in real world exhibits rate-dependent hysteresis. Rate-dependent hysteresis is a form of hysteresis which changes its hysteretic behavior when the rate or the frequency of their driving signal varies.

Fig.2.12 gives an illustrative example of rate-dependent hysteresis of the piezo electric actuator observed with the piezoelectric used in this disserta-

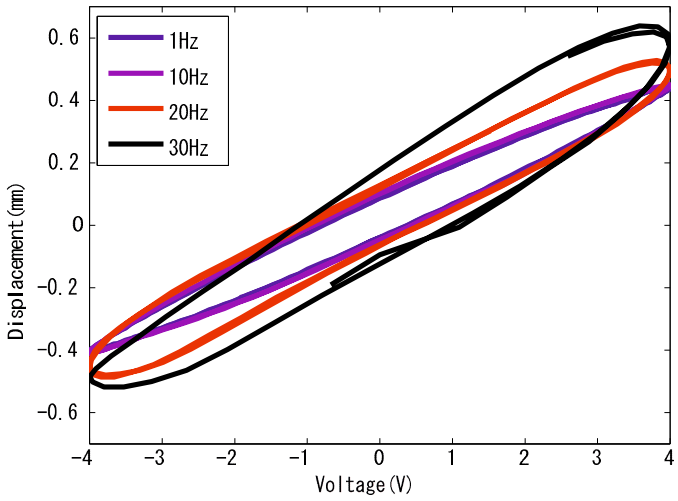

Figure 2.12 Examples of rate-dependent hysteresis of piezo electric actuator

tion. This figure contains four input/output trajectories of a single piezo actuator. The difference of the results comes from the difference in the frequency of the driving sinusoidal signals.

The lateral axis corresponds to the value of the input voltage and the vertical axis shows the displacement responses of the actuator. It can be seen that the shapes of the trajectories are completely different.

2.3 Soft Computing Tools

Compared with traditional methods, the idea and use of neural network and bio inspired algorithms give the new direction to solve the complex problems such as particle swarm optimization, genetic algorithm, membrane computing and so on.

2.3.1 Radial Basis Function Nerural Network

Radial basis function neural network (RBFNN) is one implementation of the artificial neural network that uses radial basis functions as its activation functions, which is first formulated by Broomhead and Lowe in 1988[64,65]. RBF neural network has better ability of approximating nonlinear mappings, ease of generalization, fast convergence of training process and simplicity of architecture.

The output of RBFNN is a linear combination of the values of radial basis functions to the inputs and neuron parameters. Radial basis function network can be applied to various problems, including regression, time series prediction, function approximation, classification, and system control.

The supervised learning for neural network is the problem in statistics with applications in many areas to guess or estimate a function from some example of input to output pairs with little or no knowledge of the form of the function. Fig.2.13 shows the supervised learning with neural network.

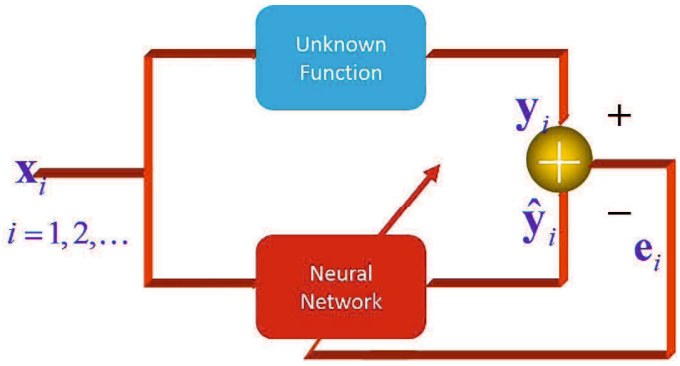

Figure 2.13 Supervised learning

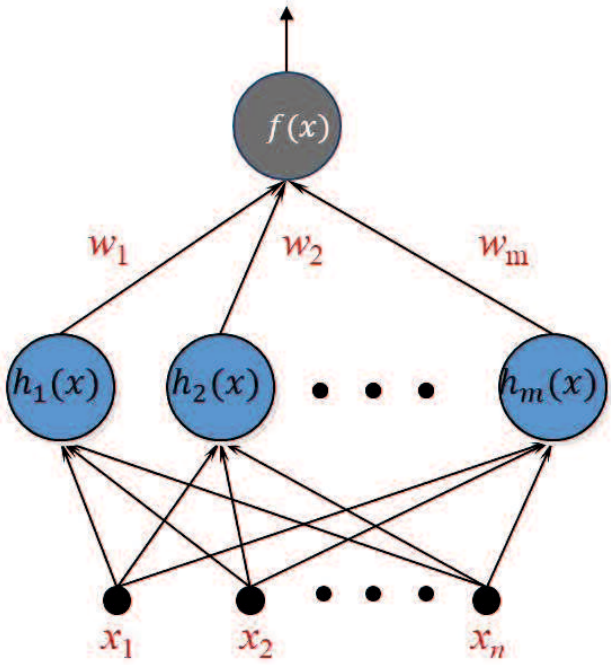

Figure 2.14 Traditional RBF neural network

Radial basis functions are a special class of function, their characteristic feature is that their response decreases or increases monotonically with distance from a central value. The center and the width are parameters of the radial basis function.

A typical radial function is the Gaussian which in the case of a scalar input is determined by

$$h(\boldsymbol{x}) = \exp\left(\frac{-\|\boldsymbol{x} - \boldsymbol{c}\|^2}{r^2}\right), \tag{2.8}$$

where center c and the width r are the parameters of RBF.

The traditional RBF neural network is shown in Fig.2.14. It shows n components of a vector $\boldsymbol{x}$ are used as the input of radial basis functions whose outputs are combined with weights w to sum up to a scalar output of the RBF neural network.

2.3.2 Particle Swarm Optimization

Particle swarm optimization denoted hereafter as PSO is an intelligent optimization algorithm proposed by Eberhart and Kennedy[66].

The PSO process begins with initializing a group of random particles corresponding to the variables to be sought, and then finds out the optimal solution through iteration. Particles track two extreme values to update their own in each iteration, one is the optimal solution called the individual extreme value p that particles themselves find, the other is the present global optimal solution called the global extreme value g that the particle swarm finds. When the two extreme values are found, the speed and the position of the particles will be updated by utilizing the equation

$$v_n = w * v_c + c_1 * r * (p - p_c) + c_2 * r * (g - p_c) \tag{2.9}$$

for the speed and

$$p_n = p_c + v_n \tag{2.10}$$

for the position of the particles, where v_n represents the new speed of the particles, v_c their current speed, p_n new position of the particles and p_c being the current position of the particles. The quantity $r(0 < r < 1)$ in Eq.(2.9) is a generated random number for increasing the randomness of particle move. c_1 and c_2 are called the acceleration constants, and w represents the inertia weight whose magnitude determines the strength of the inertial behavior.

2.3.3 Genetic Algorithm

Genetic Algorithm (GA) is the adaptive heuristic search algorithm based on the evolutionary ideas of natural selection and genetics. This heuristic is routinely used to provide useful solutions in optimization and search problems[67].

GA belongs to the large class of evolutionary algorithms, which generate solutions to optimization problems using techniques inspired by natural evolution, such as inheritance, mutation, selection, and crossover.

GA has been used in science and engineering as an adaptive algorithm for solving practical problems and as computational models of natural evolutionary systems. The algorithms represent an intelligent exploitation of a

random search used to solve optimization problems. Although randomized, GA is by no means random, instead they exploit historical information to direct the search into the region of better performance within the search space. Since in nature, competition among individuals for scanty resources results in the fittest individuals dominating over the weaker ones.

2.4 Membrane Computing

2.4.1 Introduction to Membrane Computing

Membrane computing proposed by Ghoerghe Paun is a new natural computing method inspired from the structure and function of living cells model. It is also called the P system. It is a branch of natural computing which investigates computing models abstracted from the structure, the functioning of living cells and their interactions in tissues or higher order biological structures[68].

Membrane computing or P system has been used in many fields. For instance, the framework of P system was used for modeling cellular structures which include the definition of two minimal models for the activity of mechanosensitive channels[69]. Membrane computing was used to solve difficult computational NP-complete problems in a polynomial time by creating exponentially membranes[70]. Membrane computing was also applied to the problems of optimization as membrane algorithm for a traveling salesman problem by Nishida[71]. A polynomial time membrane algorithm was used to compute approximate solutions to the instances of min storage by Leporati et al.[72].

Formally, the construction of membrane computing can be described by

$$\Pi = (V, T, C, \mu, w_1, \cdots, w_m, (R_1, \rho_1), \cdots, (R_n, \rho_n)) \quad (n \geq 1), \tag{2.11}$$

where

1) V represents the whole finite number of objects in a membrane computing,

2) T is the output,

3) C is the catalysts,

4) μ is the structure of membrane, consisting of n membranes, labeled 1 to n,

5) w_i $(i = 1, 2, \cdots, m)$ is the object in region i of the membrane structure,

6) R_i is the evolution rules associate with region i,

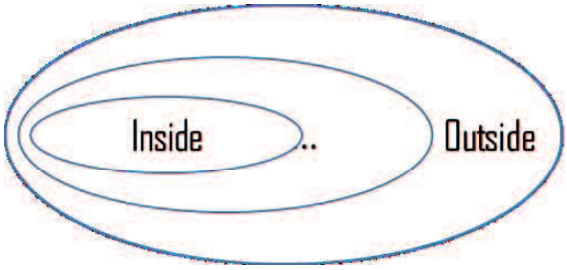

Figure 2.15 nested structure membrane algorithm

7) ρ_i is the priority for evolution rule R_i.

A membrane algorithm is first used for the NP-complete optimization problem by Nishida as an application of P system[73]. He proposed the nested structure membrane algorithm as shown in Fig.2.15. A membrane algorithm is used for optimization of control design of a ball-plate system by Liu et al[74]. They used a parallel membrane algorithm for the optimization of NN-PID controller of positioning and tracking control design of a ball-plate system.

2.4.2 Membrane Structure Genetic Algorithm

A membrane structure genetic algorithm (MSGA) is proposed in this dissertation for mathematical modeling of the rate-dependent hysteresis of piezo electric actuator, which is inspired from genetic algorithm and the structure of membrane computing.

The MSGA uses nested membrane structures, the specific rules in each membrane regions, and the transportation mechanism between the membranes. The basic idea of membrane algorithm suits well with a distributed and parallel computing device. The structure is designed in an arrangement of membranes which forms several compartments where various chemicals (objects) evolve according to computing rules. MSGA employs the rules of selection, mutation, crossover and shift as were also used in the classical genetic algorithm.

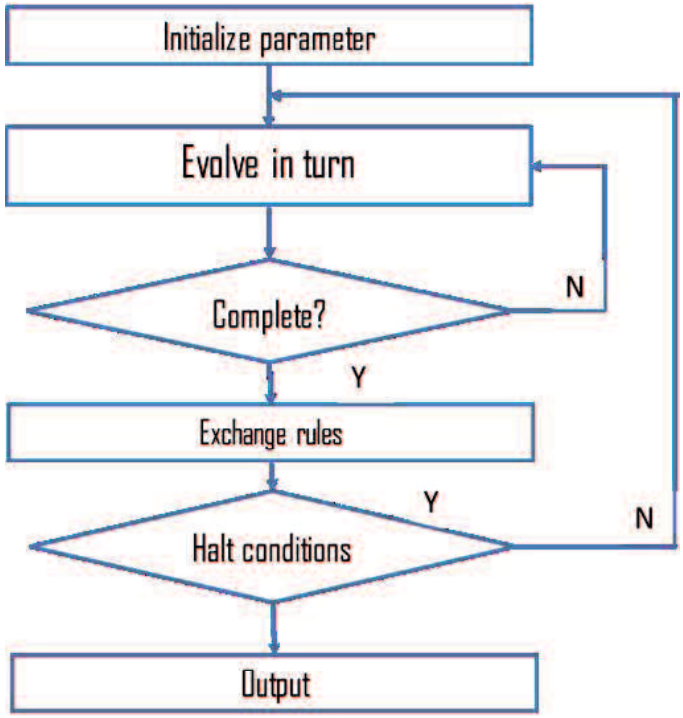

Figure 2.16 The flow chart of MSGA

In order to understand and use this membrane structure genetic algorithm, compared with genetic algorithm and particle swarm optimization, the global optimum for some testing functions have been operated.

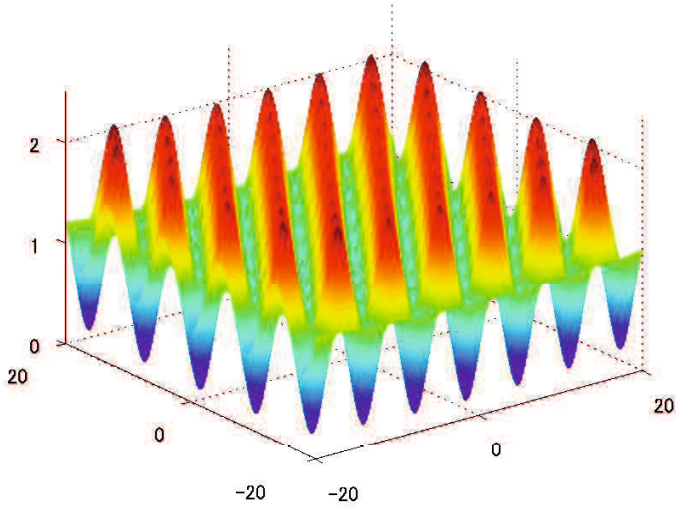

Figure 2.17 Griewank function

Fig.2.17 shows Griewank function which can be described by

$$z = \frac{1}{4000}(x^2 + y^2) - (\cos x \cos \frac{y}{\sqrt{2}}) + 1, \tag{2.12}$$

Because this function has many local minimums and they are very close to each other, it is one of the hardest functions for searching global minimum.

Fig.2.18 and Table 2.3 give the results of global optimum search of Griewank function by three algorithms. The initial objects of all the three methods are generated by random in [-600, 600] in the same condition. It can be found that the MSGA has the best result in the global optimum search of Griewank function.

Table 2.3 Optimum results of Griewank

	X	Y	Z_{min}
MSGA	-0.0051	-0.0045	0.00002
GA	-0.0568	-8.9826	0.0241
PSO	9.3242	-13.1280	0.0799

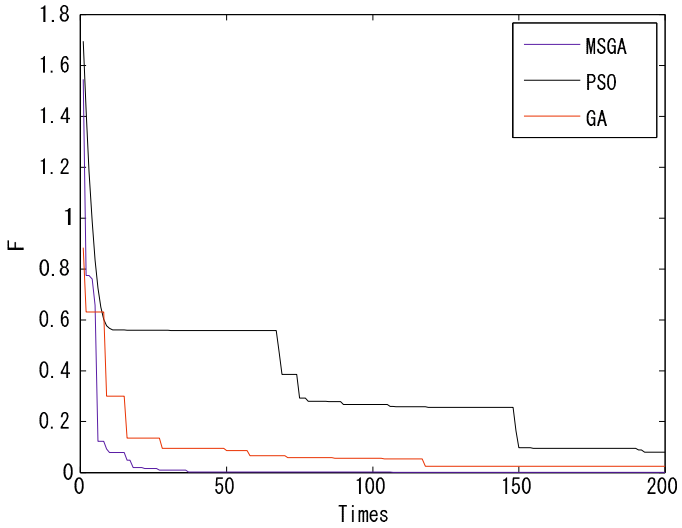

Figure 2.18 Optimum of Griewank

Another example is the Schwefel function. It is also a complex function, the global minimum is on the edge which is very close to the local minimum. Classical methods is difficult to search the global minimum of the function.

Schwefel function shown in Fig.2.19 is described by

$$z = -x \sin \sqrt{x} - y \sin \sqrt{y}, \tag{2.13}$$

Table 2.4 Optimum results of Schwefel

	X	Y	Z_{min}
MSGA	420.9711	420.9487	-837.9657
GA	421.8985	420.9203	-837.8564
PSO	411.0058	421.0312	-825.5509

Fig.2.20 and Table 2.4 give the results of global optimum search of Schwefel function by three algorithms. The initial objects of all the three methods are generated by random in [-500, 500] also in the same condition The results also show MSGA has the best result in the global optimum search of Schwefel function.

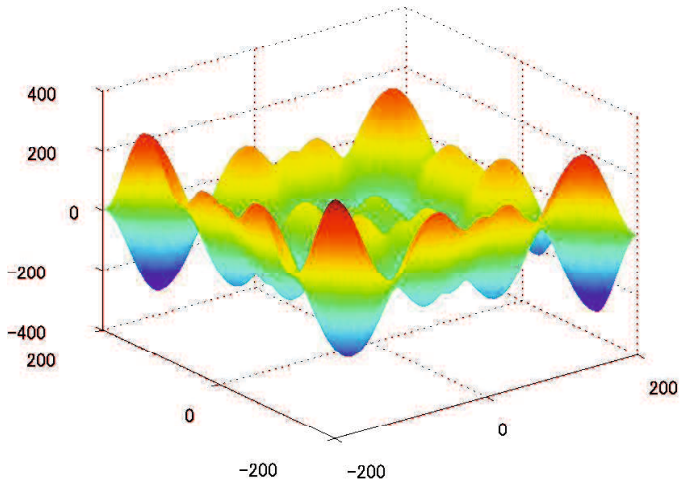

Figure 2.19 Schwefel function

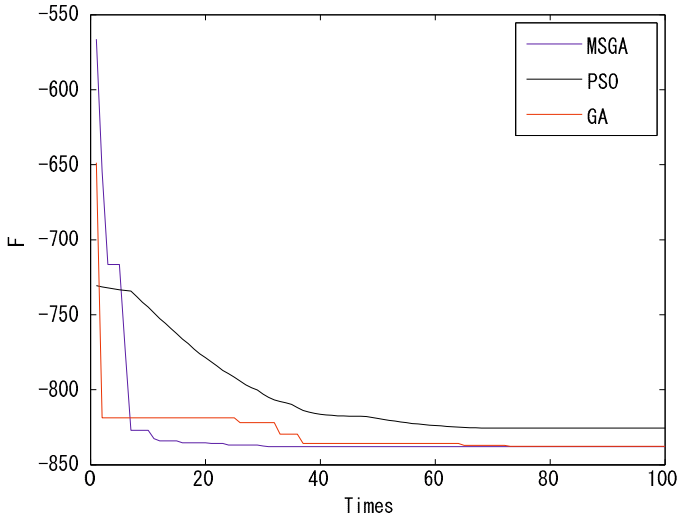

Figure 2.20 Optimum of Schwefel

The flow chart in Fig.2.16 shows the computation process of MSGA algorithm. The details of MSGA will be introduced later in this dissertation alongside with the specific content of this research.

Chapter 3

Modeling of Rate-dependent Hysteresis of Piezo Electric Actuator

3.1 Bouc-Wen Hysteresis Model for Piezo Electric Actuator

3.1.1 Hysteresis Modeling with Bouc-Wen model using Membrane Structure Genetic Algorithm Parameters Fitting

The Bouc-Wen model introduced by Bouc and extended by Wen is a good mathematical model which is capable of capturing the property of a wide class of hysteretic systems. Foregoing research[8] shows that it is sometimes necessary to modify the structure of Bouc-Wen model in order to apply it to the modeling of piezo electric actuators. However, it is presumed to be possible to apply original Bouc-Wen model for modeling the behavior of piezo electric actuator provided that an improved global optimization algorithm is used in the parameter identification.

This chapter proposes the use of the membrane structure genetic algorithm which is hereafter abbreviated as MSGA for parameter determination

of Bouc-Wen model.

The Bouc-Wen model for piezo electric actuator decomposes the output of a hysteretic component $D(t)$ into a non-hysteretic displacement $d(t)$ and a hysteretic component $h(t)$ by the equation

$$D(t) = d(t) - h(t). \tag{3.1}$$

Fig.3.1 shows the curve of hysteretic component $h(t)$ of our piezo electric actuator (d_e=0.16, d_0=0). Observed from the curve of this figure and the plots in Fig 2.13 in Chapter 2, we have decided to subtract $h(t)$ from $d(t)$ in Eq.(3.1). The non-hysteretic component of the model is described by

$$d(t) = d_e u(t) + d_0, \tag{3.2}$$

where d_e is the ratio of the displacement to the input, $u(t)$ is the input voltage and d_0 is the initial displacement.

The hysteretic component of the Bouc-Wen model $h(t)$ is characterized by

$$\dot{h}(t) = \alpha\dot{u}(t) - \beta|\dot{u}(t)||h(t)|^{n-1}h(t) - \gamma\dot{u}(t)|h(t)|^n, \tag{3.3}$$

where α, β, γ and n are the parameters of the model which govern the shape and the magnitude of hysteresis.

In order to apply Bouc-Wen model to capture the hysteretic behavior of something, the parameters of Bouc-Wen model need to be adjusted appropriately. Fig.3.2 shows the Bouc-Wen model curve corresponding to α=0.6, β=0.6, γ=0.6 and n=0.6.

In order to do the Bouc-Wen hysteresis modeling, a MSGA global optimization algorithm is proposed for parameter identification of Bouc-Wen modeling of our piezo electric actuator. The MSGA uses nested membrane structures, the rules in separated membrane regions, and the transported mechanism from the membranes. With the help of all the ingredients, the parameters fitting problem of Bouc-Wen modeling for a piezo electric actuator can be solved. Fig.3.3 depicts the proposed membrane structure of MSGA used in the parameter fitting of Bouc-Wen model to comply with the behavior of our bi-morph piezo actuator.

The structure of MSGA has 5 membranes. The membranes 1, 2, 4 are referred to as the elementary membrane. The final results of MSGA will be

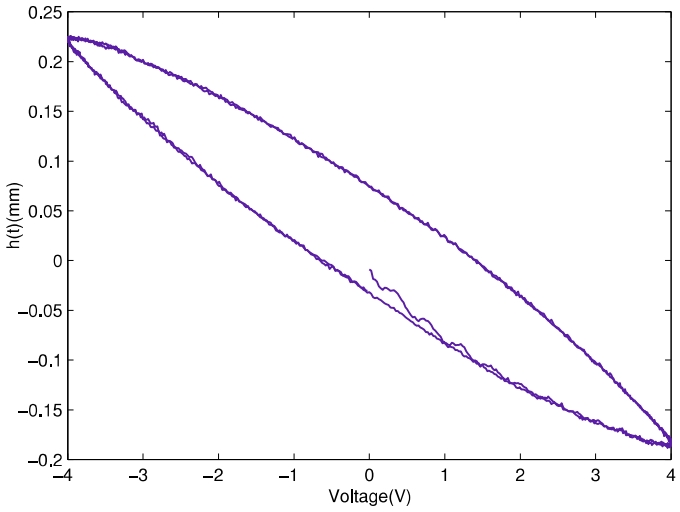

Figure 3.1 The hysteretic component h(t)

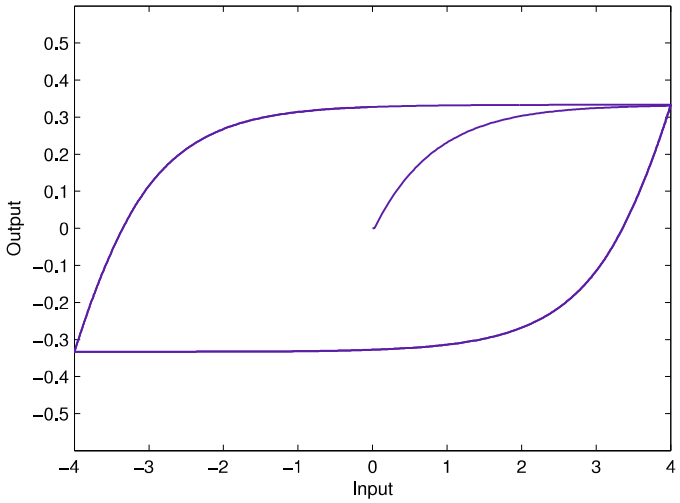

Figure 3.2 Bouc-Wen model

outputted to environment through skin. 5 membranes are utilized as the compartments of the membrane structure. Membranes include multi-sets of objects which evolve according to given rules in a synchronous non-deterministic maximally parallel manner. The process of MSGA can be organized as follows.

Step 1: Specify the total population size, the number of membranes and the subpopulation size of objects in each membrane.

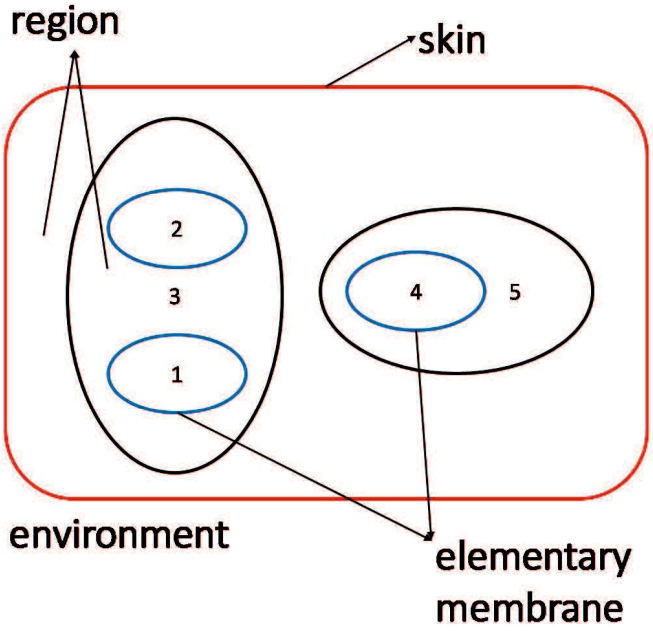

Figure 3.3 membrane structure

Step 2: Objects of each membrane utilize the evolution rules of selection, mutation, crossover and shift to obtain the fitness objects. V_i is the set of multiple objects in each membrane, V_i' is the fitness objects by operation, V_{in} is the update objects in operation and p is probability between [0,1].

Selection rules: A roulette wheel approach is adopted as the selection procedure, which is one of the fitness-proportional selection. In this scheme a new V_{in} is selected by roulette wheel selection operator, the probability of selection is proportional to the value of fitness.

$$\begin{cases} V_i' = V_i \quad (f_n \leq f_i) \\ V_i' = V_{in} \quad (f_n \geq f_i) \\ p_s = \dfrac{f(V_i)}{\sum_1^{Size} f(V_i)} \end{cases} \tag{3.4}$$

where p_s is the probability of selection, f is the value of fitness, the symbol f_n represents the fitness of new V_{in} and f_i is the fitness of V_i.

Mutation rules:

$$\begin{cases} V_i = (v_{i1}, v_{i2}, \cdots, v_{in}) \\ v'_{in} = \eta \quad (p_m \geq p) \\ V'_i = (v'_{i1}, v'_{i2}, \cdots, v'_{in}) \end{cases} \tag{3.5}$$

where η is the mutation variation, p_m represents the probability of mutation.

Crossover rules:

$$\begin{cases} V_1 = (v_{11}, v_{12}, \cdots, v_{1n}) \\ V_2 = (v_{21}, v_{22}, \cdots, v_{2n}) \\ V'_1 = \alpha V_1 + (1-\alpha) V_2 \quad (p_c \geq p) \end{cases} \tag{3.6}$$

where α is a random factor set between [0,1] and p_c represents the probability of crossover.

Shift rules:

$$\begin{cases} V_i = (v_{i1}, \cdots, v_{ia}, v_{ib}, \cdots, v_{in}) \\ V'_i = (v_{i1}, \cdots, v_{ib}, v_{ia}, \cdots, v_{in}) \quad (p_s \geq p) \end{cases} \tag{3.7}$$

where p_s represents the probability of shift.

Step 3: When the evolution is over, the communication rule of MSGA is activated to exchange the fitness objects among the membranes. The communication rule is employed to obtain the optimal objects among all the membranes after the evolution rules are applied to obtain better objects in each membrane region.

Step 4: Output the optimal parameters $(d_e, \alpha, \beta, \gamma, n)$ to our Bouc-Wen model.

MSGA is primarily divided into four steps as shown in the flowchart in Chapter 2: input, evolution, communication and the output. We have applied proposed MSGA is to parameters identification of Bouc-Wen hysteresis modeling. The initial sets necessary for MSGA include the number of initial objects of each membrane, the probabilities of evolution rules, the percentage of communication, the number of iterations and some parameters.

The number of initial objects of each membrane is set to be 40 (totally 200) which consist of the parameters d_e, α, β, γ and n. The initial parameters are shown in Table 3.1, where G is the maximum number of iterations,

p_m represents the probability of mutation, p_c represents the probability of crossover, p_s represents the probability of shift, and p denotes the percentage of communication. The elements of initial objects in each membrane are randomly generated in [0,1.5]. Each object is a vector of the parameters of Bouc-Wen model which has different influence and contribution to the output of Bouc-Wen model. Every object in the membrane will be assigned a fitness value which shows the ability of the specific object to adapt to the environment. Actually, the better the object is, the higher the its fitness value is.

Table 3.1 The initial parameters setting of MSGA

G	p_m	p_c	p_s	p
200	0.1	0.9	0.05	30%

In order to visualize the progress of Bouc-Wen modeling based on MSGA, the instantaneous fitting error function at discrete time k defined by

$$g[k] = \frac{|y(k) - y_m(k)|^2}{2} = \frac{e(k)^2}{2} \tag{3.8}$$

is used, where y is the output displacement of piezo electric actuator obtained in the experiment and y_m is the output of Bouc-Wen model which corresponds to the current best individual model. Accumulated error for a single iteration is defined by

$$J = \sum_{k=1}^{N} g(k) \tag{3.9}$$

Equation (3.9) is calculated over one specific iteration where N represents the number of signal samples contained in a single iteration.

3.1.2 Results of Bouc-Wen Modeling for Piezo Electric Actuator

The value of J under the 1[Hz] sinusoidal excitation experimental data can be observed from Fig.3.4. Classical GA is used as a comparison for MSGA, the

initial setting of GA is the same with MSGA. It shows that MSGA provides both faster convergence and better fitting results than GA.

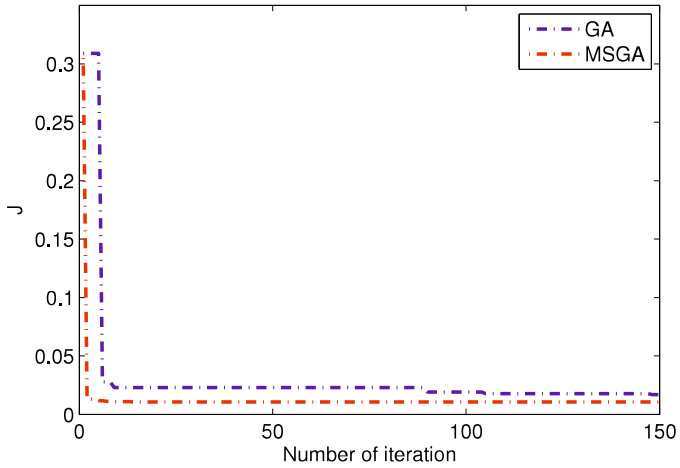

Figure 3.4 The progress of parameters identification

Table 3.2 RMS error by different identification method

	GA	MSGA
1Hz	0.0145[mm]	0.0066[mm]
10Hz	0.0451[mm]	0.0286[mm]
20Hz	0.0635[mm]	0.0439[mm]
28Hz	0.0974[mm]	0.0543[mm]

Fig.3.5, 3.7, 3.9 and 3.11 give the measured output displacement of piezo electric actuator and the output displacement of the Bouc-Wen model based on MSGA and classical GA.

The output displacement data of piezo electric actuator under sinusoidal excitation is used to identify the parameters of Bouc-Wen model, Model outputs with MSGA and GA for the same input signal are plotted in Figs.3.5(a), 3.7(a), 3.9(a) and 3.11(a), together with the corresponding actual motion of the actuator. Corresponding modeling errors are given respectively in Fig.3.5(b), 3.7(b), 3.9(b) and 3.11(b).

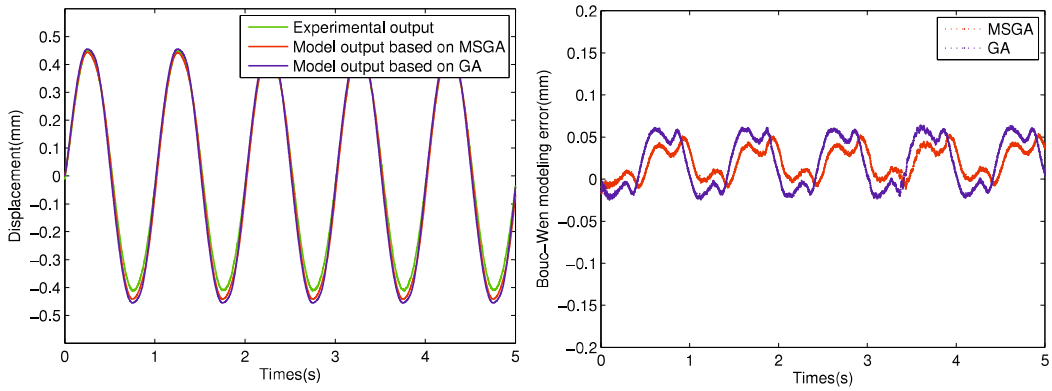

(a) $y(k)$ and $y_m(k)$ (b) Modeling error

Figure 3.5 The output displacement of sinusoidal input excitation under 1[Hz]

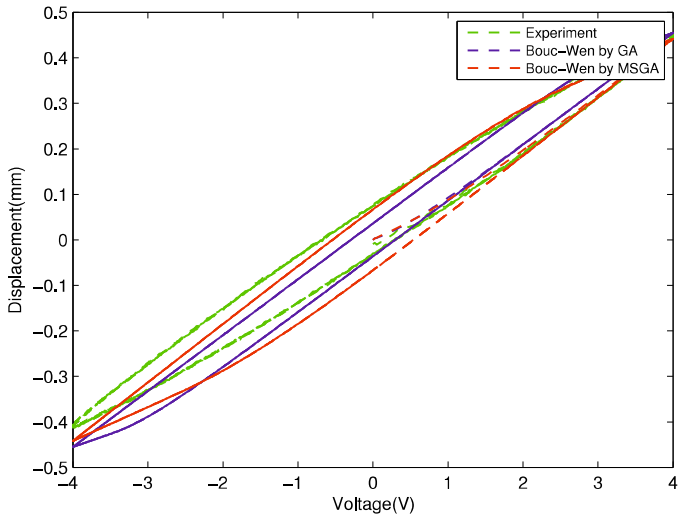

Figure 3.6 Hysteresis performance under 1[Hz]

It can be found the results of Bouc-Wen modeling based on MSGA is better than the one obtained with classical GA. The RMS error of Bouc-Wen modeling based on these two identification algorithms are given in Table 3.2. Observing Table 3.2, under the 1[Hz] sinusoidal excitation, RMS modeling error of the MSGA model is 0.0066[mm], whereas RMS modeling error of GA model is 0.0145[mm]. Thus the difference is not so obvious. However, as the frequency increases, responses of MSGA trained model under 10, 20 and 28[Hz] are much better than the GA-trained model for Bouc-Wen model. It can be seen that the Bouc-Wen model based on MSGA perform better at high input frequencies. The hysteresis performance under different input

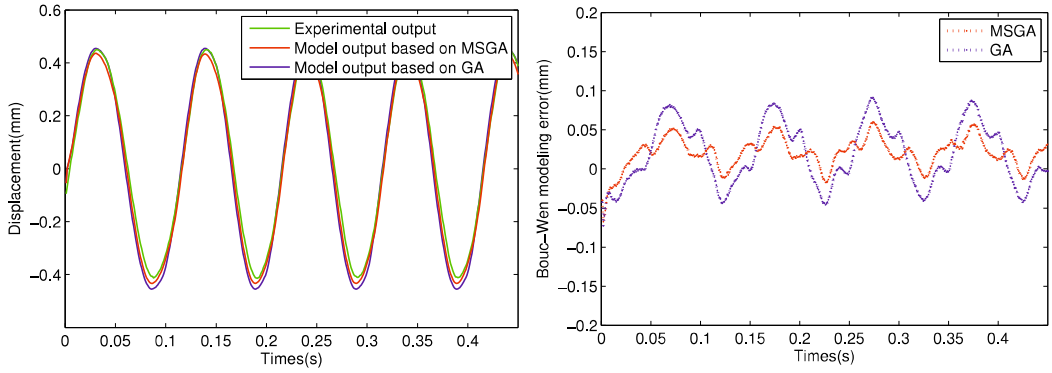

(a) $y(k)$ and $y_m(k)$ (b) Modeling error

Figure 3.7 The output displacement of sinusoidal input excitation under 10[Hz]

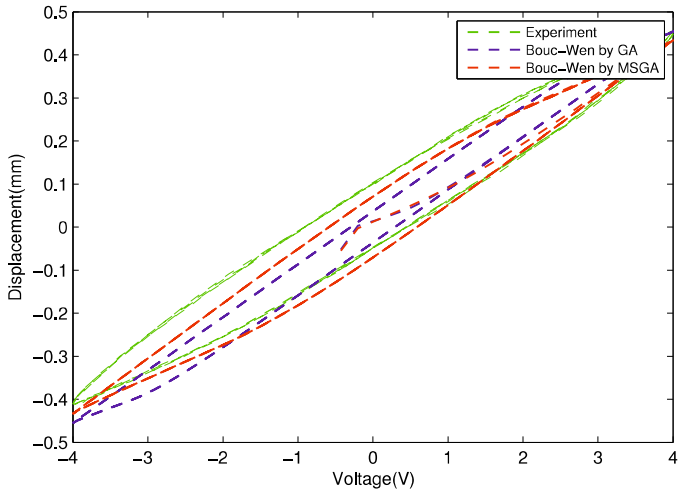

Figure 3.8 Hysteresis performance under 10[Hz]

frequencies of our piezo electric actuator and Bouc-Wen model are shown in Fig.3.6, 3.8, 3.10 and 3.12, the window of time of all there figures follow the time of output. It can be found that the Bouc-Wen model can almost capture the properties of hysteresis of the piezo electric actuator, but some errors remain at the maximum and minimum of Bouc-Wen model output which may result from the structural error of the Bouc-Wen model used for our piezo actuator, the accuracy of hysteresis modeling by Bouc-Wen model is not good enough. Improving the Bouc-Wen model expression may help to improve the results which we will continue our research on this topic. In order to get more precise modeling, we established another model for

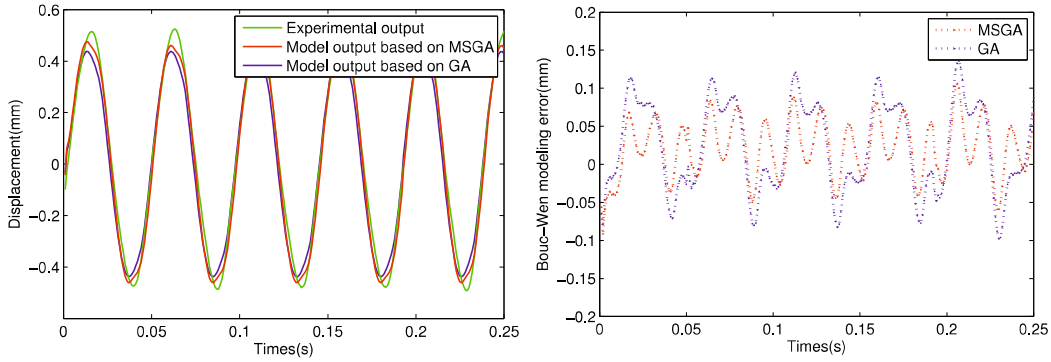

(a) $y(k)$ and $y_m(k)$ (b) Modeling error

Figure 3.9 The output displacement of sinusoidal input excitation under 20[Hz]

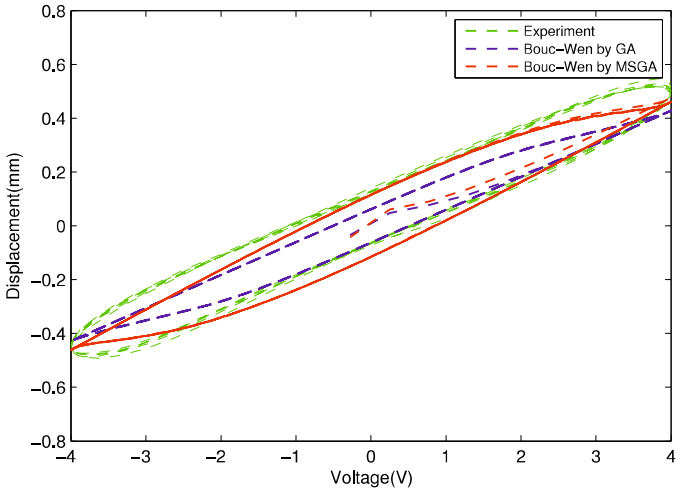

Figure 3.10 Hysteresis performance under 20[Hz]

hysteresis modeling of piezo electric actuator.

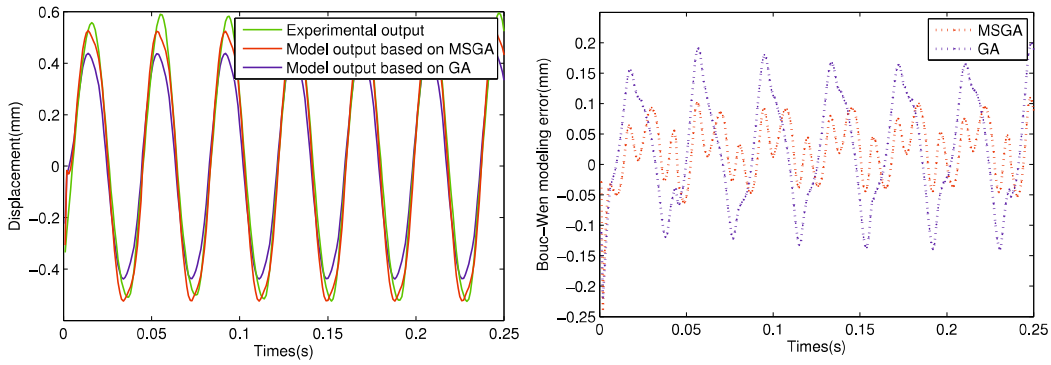

(a) $y(k)$ and $y_m(k)$ (b) Modeling error

Figure 3.11 The output displacement of sinusoidal input excitation under 28[Hz]

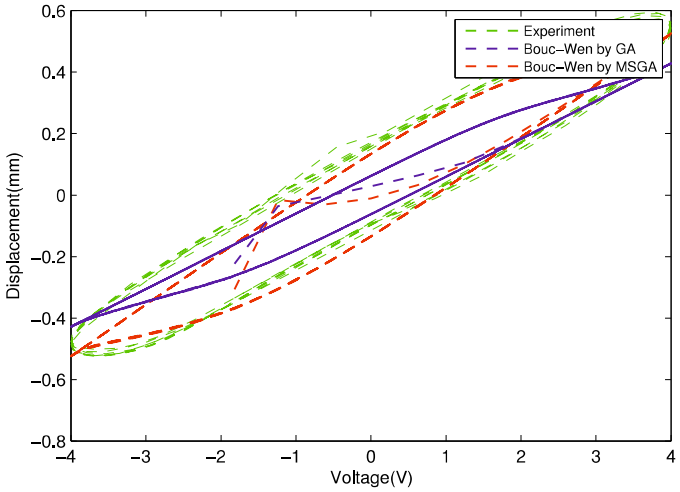

Figure 3.12 Hysteresis performance under 28[Hz]

3.2 RBFNN Hysteresis Model for Piezo Electric Actuator

3.2.1 Structural Description of RBFNN Model for Rate-dependent Hysteresis of Piezo Electric Actuator

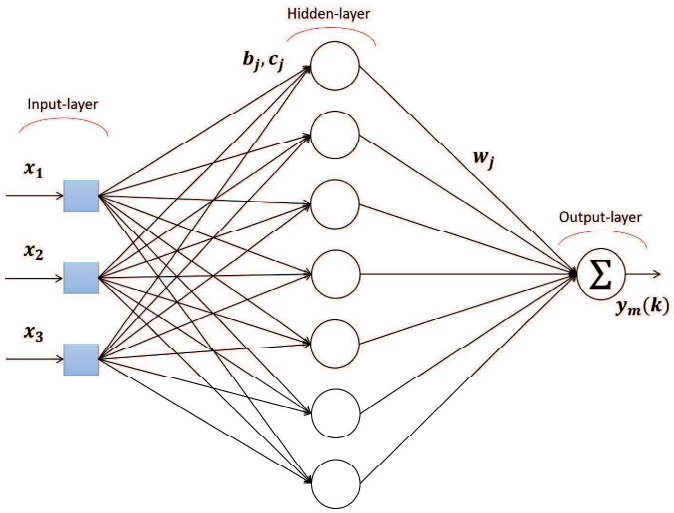

Figure 3.13 Structure of RBFNN model

Neural network is a very powerful tool for nonlinear mapping, and RBF neural network has better ability of approximating nonlinear mappings, ease of generalization, fast convergence of training process and simplicity of architecture. Therefore, RBF Neural network is a very good tool for hysteresis modeling. Due to multi-valued nature of hysteresis nonlinearity, a three layered neural network with radial-basis activation functions has been applied here for modeling piezo actuator hysteresis. The network is configured to have a 3-7-1 structure as described in Fig.3.13. The quantities labeled x_1, x_2 and x_3 are fed to the input nodes. These correspond to

$$\begin{aligned} x_1 &= r(k) \\ x_2 &= r(k-1) \\ x_3 &= y(k-1) \end{aligned} \tag{3.10}$$

respectively, where $r(k)$ represents the value of the training input signal at time k, $r(k-1)$ being the value of the training signal at previous time instant and $y(k-1)$ amounts to the previous output displacement of the actuator.

The choice of variables described by Eq.(3.10) amounts to the introduction of the nonlinear ARMA model structure for modeling rate-dependent hysteresis. This set of inputs corresponds to the simplest model which has the lowest model order among all.

Nodes at hidden layer utilize multiple radial basis function units necessary to capture the input-output dynamics of piezo electric actuator. Let $\boldsymbol{x}_i(k)$ denote the vector of input signal sequence at time k defined by

$$\boldsymbol{x}_i(k) = [x_1, x_2, x_3]^T. \tag{3.11}$$

The output of the j-th hidden layer node $h_j(k)$ is calculated accordingly by

$$h_j(k) = \exp\left(\frac{-\|\boldsymbol{x}_i(k) - \boldsymbol{c}_j\|^2}{2b_j^2}\right), \quad (j = 1, 2, \cdots, 7), \tag{3.12}$$

where

$$\boldsymbol{c}_j = [c_{1j}, c_{2j}, c_{3j}], \quad (j = 1, 2, \cdots, 7) \tag{3.13}$$

represents the center of Gaussian RBF function and the scalar constant b_j amounts to its Gaussian width. The output of RBF neural network model denoted as $y_m(k)$ in the figure is calculated accordingly by

$$y_m(k) = \sum_{j=1}^{7} w_j \cdot h_j(k), \tag{3.14}$$

where w_j is the weight corresponding to $h_j(k)$.

In addition, although it is possible to introduce more hidden layer nodes to this model, adding more hidden nodes will result in the excess redundancy and the amount of computation which should be avoided in the real time control implementation. In order to see how the number of nodes of input layer and hidden will influence the results of the hysteresis modeling, we have tried more experiments with more nodes of input and hidden layers in the experiments of next part.

3.2.2 Training RBFNN Model Using PSO

Training parameters in RBFNN to capture input-output behavior of piezo actuator can be thought as doing the model identification task in the classical

approach of model based control system design. It is important to have a reliable, high precision model in order to achieve high control performance, no matter how the model is constructed. The particle swarm global optimization (PSO) algorithm which is proposed by Eberhart and Kennedy is used for Training RBFNN model here.

The process of PSO algorithm begins with initializing a group of random particles corresponding to the parameters to be optimized, then finds out the optimal solution through iteration. Particles track two extreme values to update their own in each iteration One is the optimal solution called the individual extreme value p that particles themselves find, and the other is the present global optimal solution called the global extreme value g that the particle swarm finds. When the two extreme values are found at each iteration, the speed and the position of the particles will be updated by

$$v_n = w \times v_c + c_1 \times r \times (p - p_c) + c_2 \times r \times (g - p_c) \tag{3.15}$$

for the speed, and

$$p_n = p_c + v_n \tag{3.16}$$

for the position of the particles, where v and p amount to the speed and position of a particle respectively, with suffix n representing the *new* updated values and c being their *current* values. The quantity $r(0 < r < 1)$ in Eq.(3.15) is a randomly generated number to increase randomness of particle move. $c_1(= 2)$ and $c_2(= 2)$ are called the acceleration constants, and w represents the inertia weight whose magnitude determines the strength of the inertial behavior.

The parameters c_j, b_j and w_j of RBFNN model in Eqs.(3.12) and (3.14) will be tuned by the PSO algorithm during the training calculation as described, and the RBFNN model will be trained to provide the output value $y_m(k)$ at k-th sampling instant which is expected to be identical to the actuator output displacement $y(k)$ as schematically shown in Fig.3.14, where the signal $r(\cdot)$ in the figure represents the input signal for training RBF neural network, two past signal inputs are applied to the RBF neural network model.

Training of RBFNN will be conducted by PSO to minimize the instantaneous fitting error function defined by

$$g(k) = \frac{|y(k) - y_m(k)|^2}{2} = \frac{e(k)^2}{2}, \tag{3.17}$$

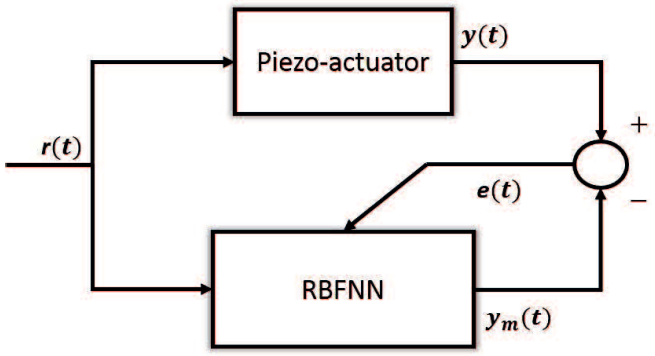

Figure 3.14 RBF neural network modeling

where $y(k)$ is the actuator output and $y_m(k)$ is the RBFNN model output both at time k. The parameters to be trained with PSO in the 3-7-1 RBFNN actuator model include the center vector $\boldsymbol{c}$ and widths of function b at hidden layer, and the weights w_j in the output equation Eq.(3.14).

3.2.3 Results of RBFNN Modeling for Piezo Electric Actuator

Before conducting the identification of real world piezo electric actuator dynamics, a numerical practice has been conducted to illustrate the performance of RBFNN modeling. Based on the algorithm which has been introduced above, a 20[Hz] sinusoidal voltage signal is utilized as a training input. In the *numerical* identification setup, the output $y[k]$ is determined by

$$y[k] = 0.9802y[k-1] - 0.3406r[k] + 0.3306r[k-1], \tag{3.18}$$

where $r[k]$ is the aforementioned sinusoidal input. We used this description to operate virtual identification first, then the actual actuator output measurement was used in the *experimental* identification. The ordinary back propagation (BP) algorithm, in addition to PSO training, has also been adopted to train RBFNN for both these two setups to illustrate the outstanding optimization performance of PSO. The number of initial population is selected to be 100, individuals length to be 35 and the maximum number of iterations to be 100, each of which is determined by experience. When model output y_m approaches to the real actuator response y, g must decrease gradually.

Fig.3.15 to Fig.3.18 show the results of model identification in the *numer-*

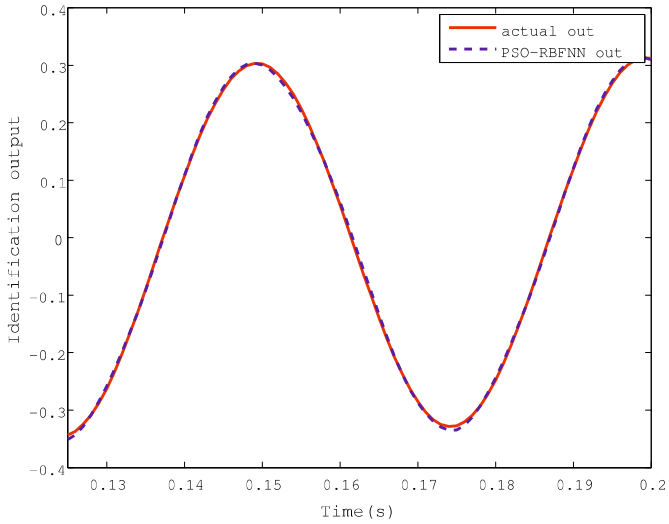

Figure 3.15 Numerical output results $y[k]$ and $y_m[k]$ trained by PSO

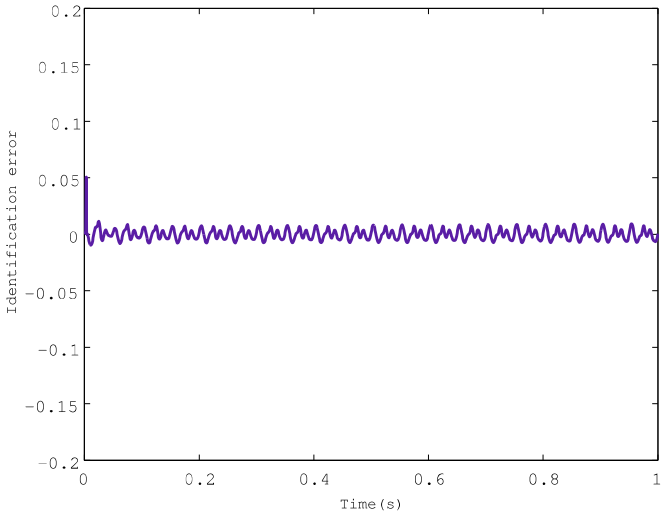

Figure 3.16 Modeling error by PSO

ical setup. Fig.3.15, Fig.3.16 correspond to the results obtained with PSO training while Fig.3.17, Fig.3.18 represent the results with Back Propagation training. The modeling error plot in Fig.3.16 and Fig.3.18 clearly show that RBFNN trained by PSO has achieved much better modeling accuracy than the one obtained with BP training.

It then proceeds to the model identification of RBFNN using the real

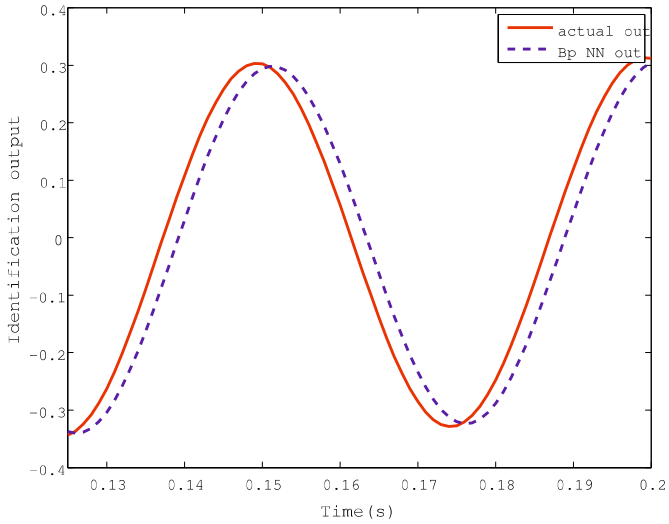

Figure 3.17 Numerical output results $y[k]$ and $y_m[k]$ trained by BP

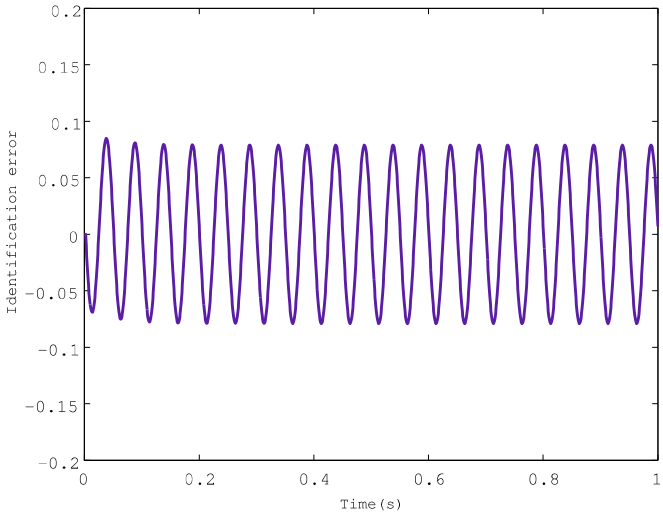

Figure 3.18 Modeling error by BP

experimental data which is acquired by driving the piezo electric actuator with 4[Hz] sinusoidal input signal. Fig.3.19 to Fig.3.22 summarize the results. These figures clearly show that output of RBFNN trained by PSO in Fig.3.20 is almost identical to the output of the piezo actuator, whereas apparently large errors can be observed in Fig.3.22 which s tuned with classical back propagation method.

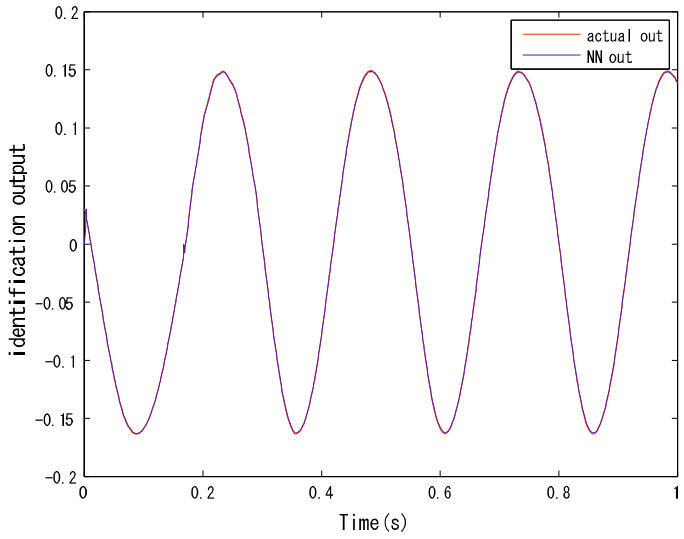

Figure 3.19 Experimental output results $y[k]$ and $y_m[k]$ trained by PSO

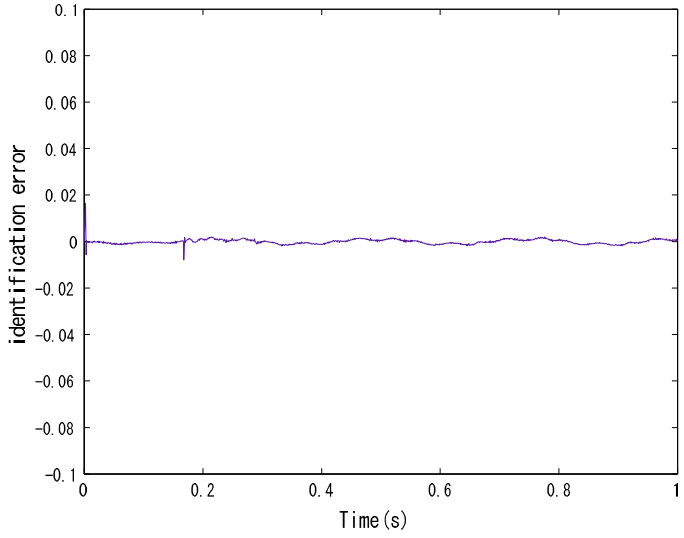

Figure 3.20 Modeling error by PSO

In order to see how the number of nodes of input and hidden layer will influence the results of the hysteresis modeling, the number of input nodes is increased to 7 which was tested as an alternate model structure first, the results are shown in Figs.3.23 and 3.24, then the number of hidden layer is increased to 9, the results are summarized in Figs.3.25 and 3.26. Compared with the results of Figs.3.19 and 3.20, the performance has little difference, setting more input nodes to the RBFNN will not contribute much to the

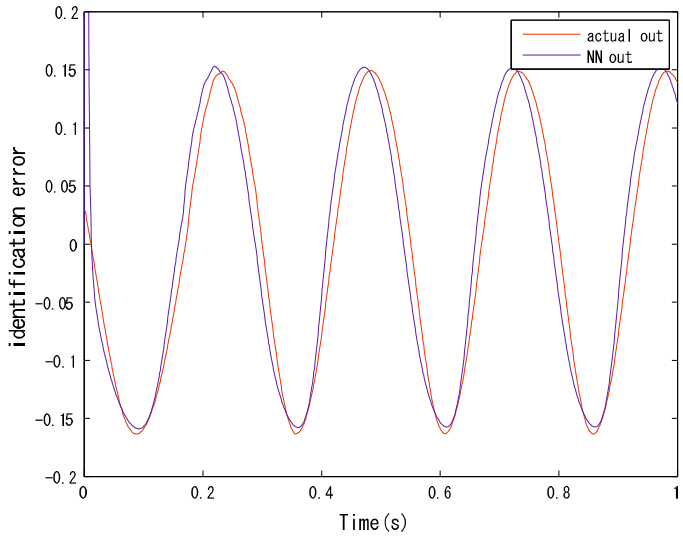

Figure 3.21 Experimental output results $y[k]$ and $y_m[k]$ trained by BP

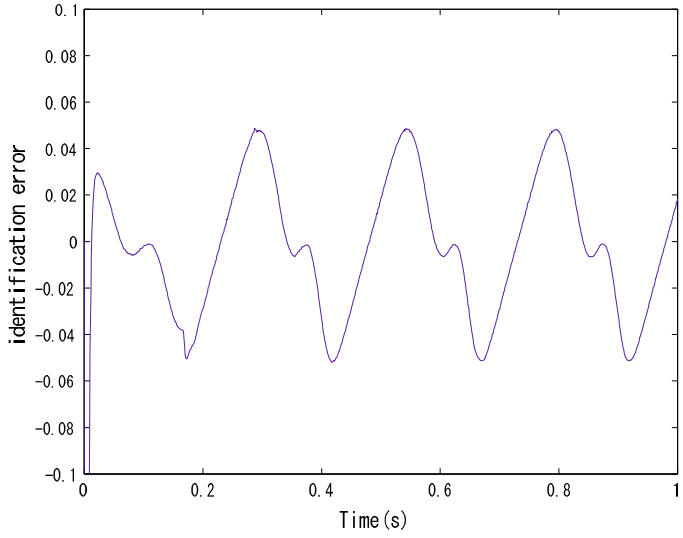

Figure 3.22 Modeling error by BP

improvement of modeling accuracy and additional nodes of hidden layer also will not contribute much to performance of our test.

After finishing the experiment of RBFNN hysteresis modeling of piezo electric actuator with particle initial population being 100, individual length 35 and the maximum number of iterations to be 100 above, another attempt of RBFNN hysteresis modeling have been generated, the initial particle of

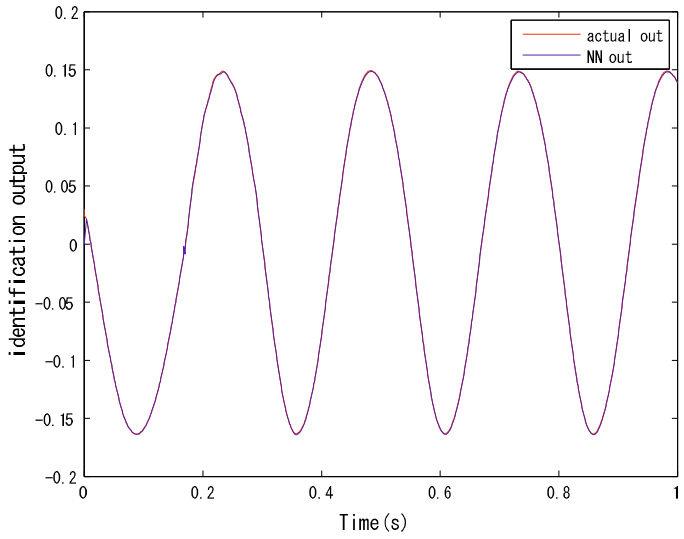

Figure 3.23 Experimental output results $y[k]$ and $y_m[k]$ trained by PSO when increasing input nodes

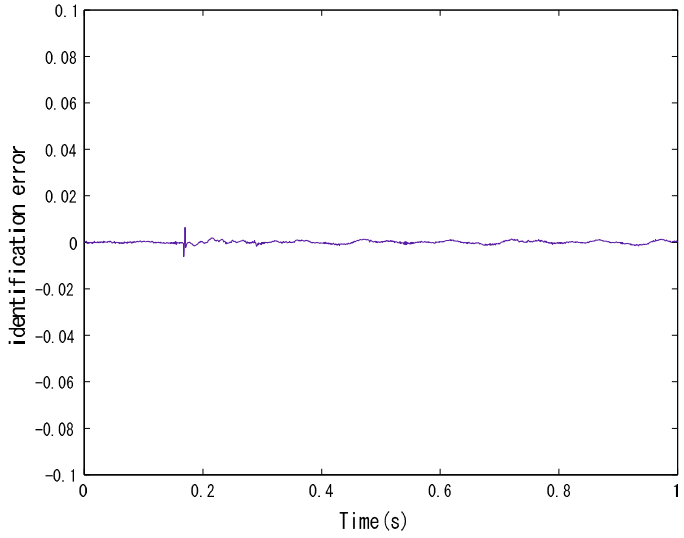

Figure 3.24 Modeling error by PSO when increasing input nodes

this experiment is set to be 150 while allowing 200 iterations, which will be shown as follows to acquire improved hysteresis modeling accuracy.

The input voltage plotted with a blue solid line in Fig.3.27(a) is the input voltage generated for training RBFNN model, and response of the actuator for this input can also be found with a red solid line in Fig.3.27(a).

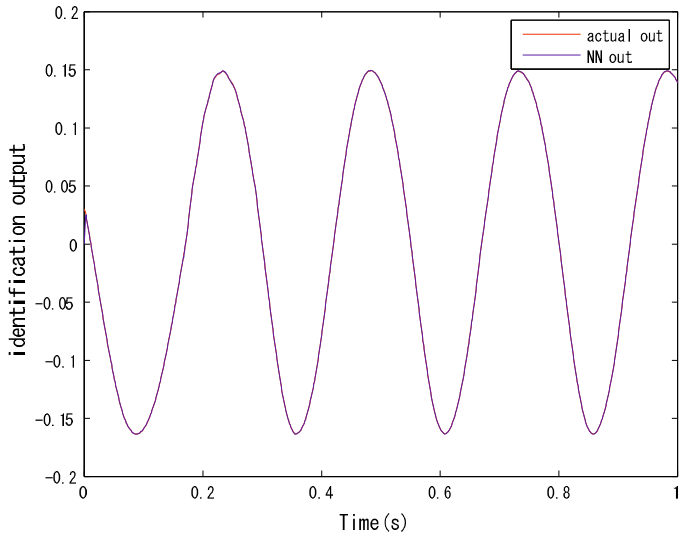

Figure 3.25 Experimental output results $y[k]$ and $y_m[k]$ trained by PSO when increasing hidden nodes

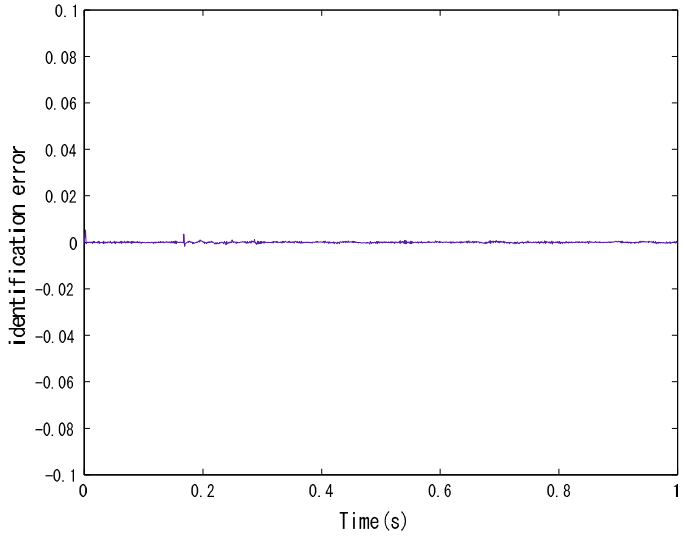

Figure 3.26 Modeling error by PSO when increasing hidden nodes

Once the parameter fitting was completed, another different input signal shown in Fig.3.27(b) was given to the actuator for parameter validation. The validation input is a time varying amplitude sinusoidal signal whose frequency also varies with time from 10 to 1[Hz]. The frequency of the voltage signal is altered to capture the property of rate-dependent hysteresis.

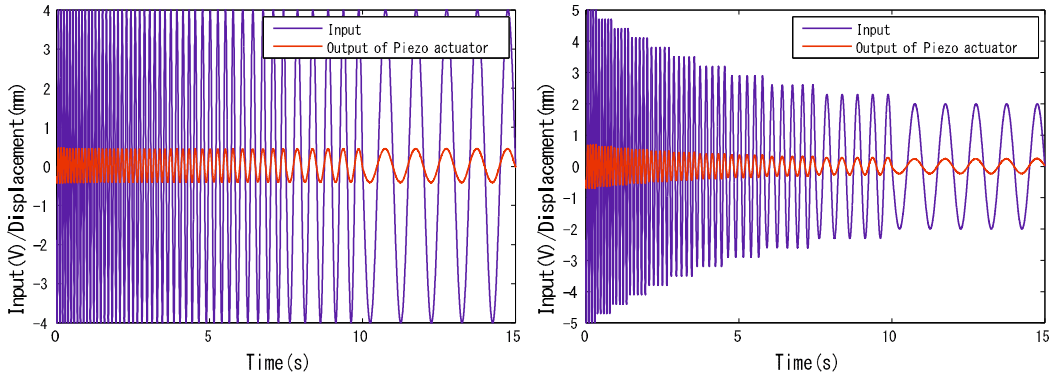

(a) Identification data of piezo actuator

(b) Validation data of piezo actuator

Figure 3.27 Input and output signals for training and validation

Figure 3.28 shows how optimization proceeds with PSO and BP. The vertical axis shows the value of the function

$$L = \sum_{k=1}^{N} g(k). \tag{3.19}$$

This function accumulates instantaneous fitting error $g(k)$ defined by Eq.(3.17) over a single learning iteration, where N is the number of signal samples contained in it. The value of L is expected to decrease as iteration number increases. It can be observed from the figure that training result is good and the proposed neural network has been trained to represent the dynamic relation between the input and the output signal of the piezo actuator, for a given range of frequency.

In order to see how learning algorithm would affect the modeling performance, another 3-7-1 RBFNN is trained with ordinary back propagation (BP) algorithm using the same dataset. The actual response of piezo actuator is depicted in the *input vs output* form as shown in Fig.3.29, it can be seen that the trajectory of hysteresis changes with both amplitude and frequency of the input voltage.

Fig.3.30 corresponds to the results of back propagation learning after 50 iterations, whereas Fig.3.31 corresponds to the results of PSO training. Fig.3.32 shows the result of additional 50 learning iterations for BP.

It can be found from the results clearly that allowing more iterations will actually improve the modeling accuracy when BP is used for learning,

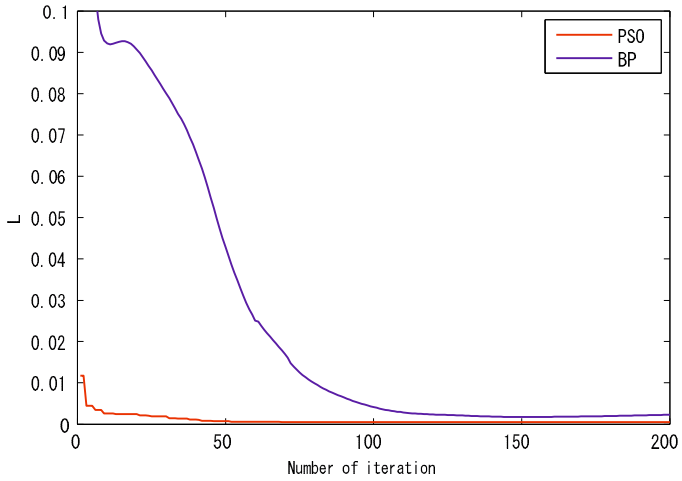

Figure 3.28 Progress of Training

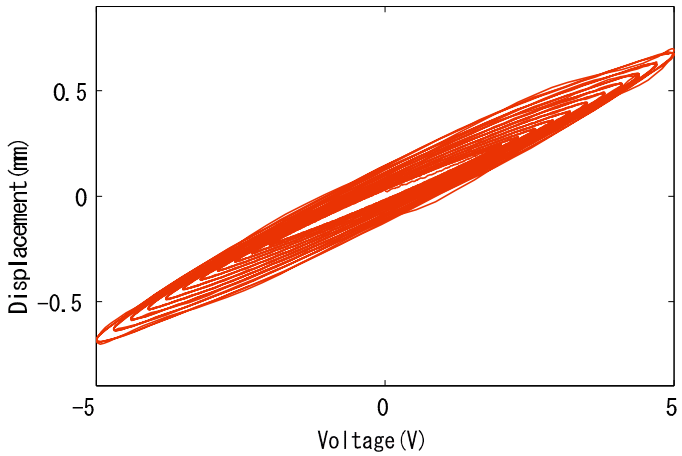

Figure 3.29 Response of the actuator to the validation input signal sequence

but it is not good enough to capture rate-dependent hysteresis of the actuator. Comparison of these figures immediately shows that RBFNN trained with PSO has successfully captured rate-dependent hysteresis of an actuator, while RBFNN trained with back propagation fails and cannot model dynamic behavior of rate-dependent hysteresis. Table 3.3 summarizes the modeling accuracy quantitatively.

In addition, we attempted another experimental verification of RBFNN modeling trained by PSO for piezo electric actuator with 10 and 20[Hz] driving signals, and the responses of RBFNN model are shown in Figs.3.33 and 3.35, whereas the modeling errors are depicted in Figs.3.34 and 3.36.

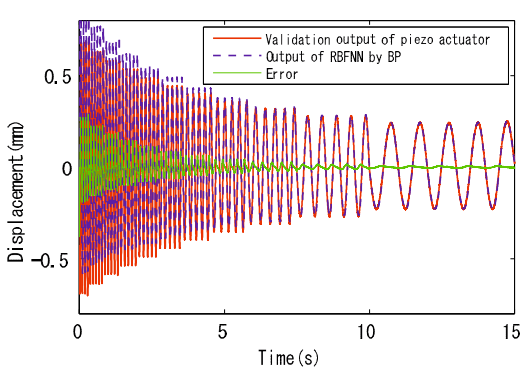

(a) RBFNN model output by BP

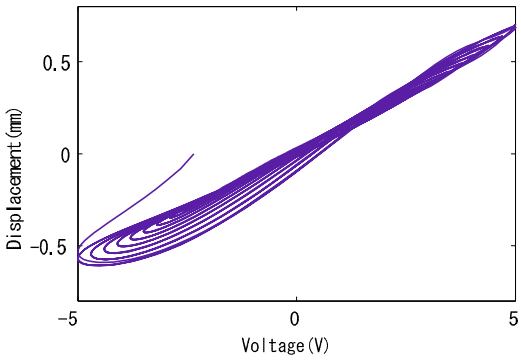

(b) Input/Output trajectory of the RBFNN model trained with BP

Figure 3.30 RBFNN modeling results trained by BP after 50 iterations

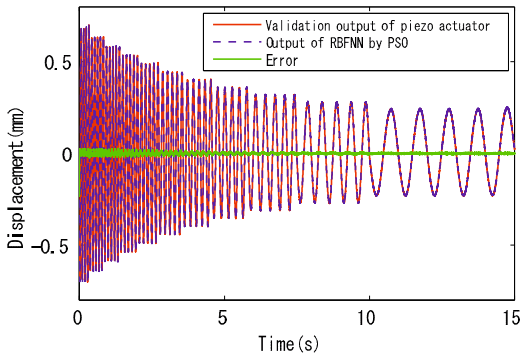

(a) RBFNN model output by PSO

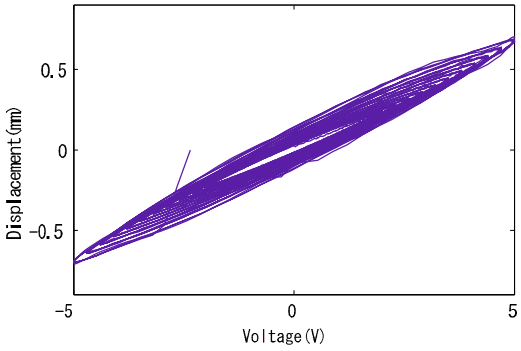

(b) Input/Output trajectory of the RBFNN model trained with PSO

Figure 3.31 RBFNN modeling results trained by PSO after 50 iterations

Table 3.3 Comparison of modeling accuracy for two differently configured RBFNNs after 50 iterations

	Max error occurred	RMS error
PSO trained model	0.027[mm]	0.003[mm] (0.5%)
BP trained model	0.2877[mm]	0.0451[mm] (8.3%)

These figures demonstrate that the model is good enough when the actuator is driven with 10[Hz] signal whereas slight degradation of accuracy is observed in 20[Hz] results. To the best of the authors' understandings, it

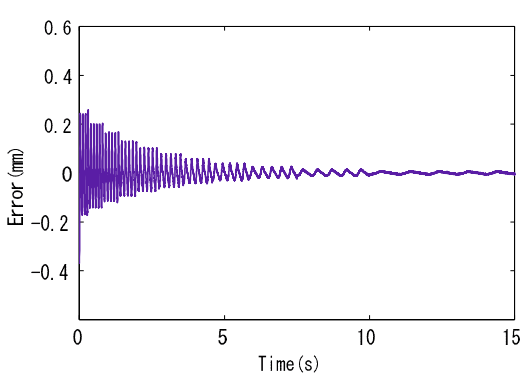

(a) Modeling error by BP

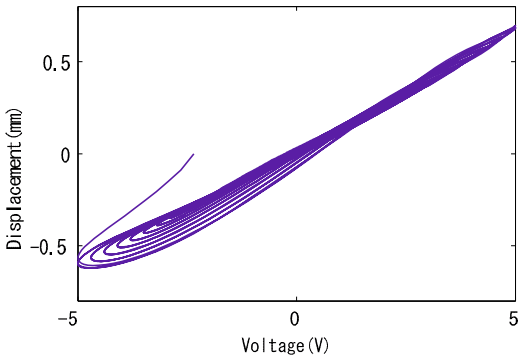

(b) Input/Output trajectory of the RBFNN model trained with BP

Figure 3.32 Results trained by BP after 100 iterations

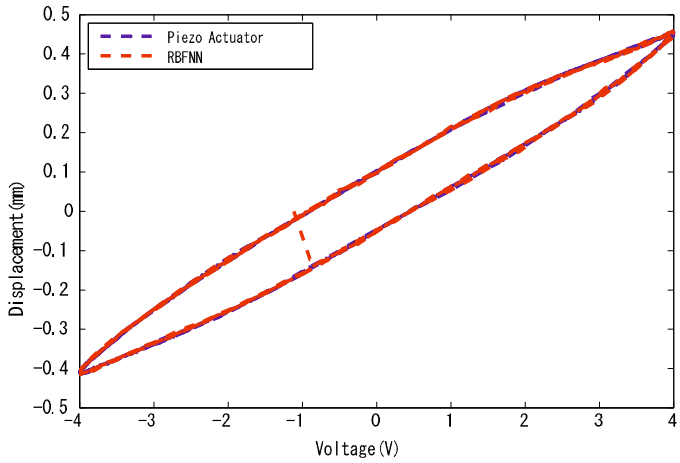

Figure 3.33 Experimental verification of RBFNN model for piezo-actuator with 10[Hz] driving signal

might be caused by the structural oscillation of the actuator which is commonly observed for 16[Hz] or above driving frequency.

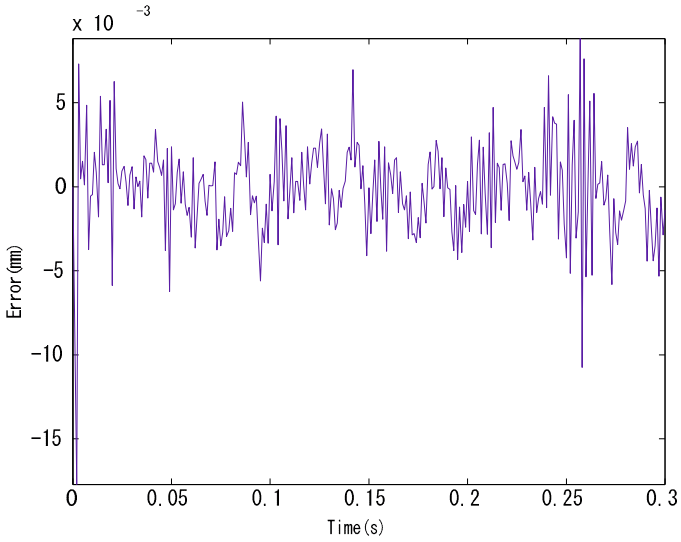

Figure 3.34 RBFNN modeling error with 10[Hz] driving signal

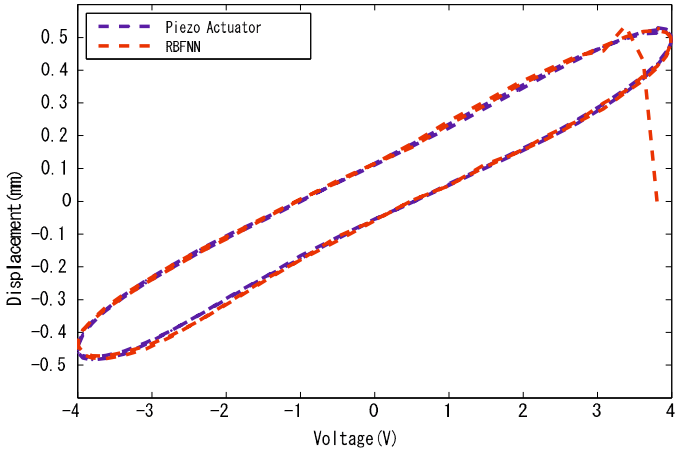

Figure 3.35 Experimental verification of RBFNN model for piezo-actuator with 20[Hz] driving signal

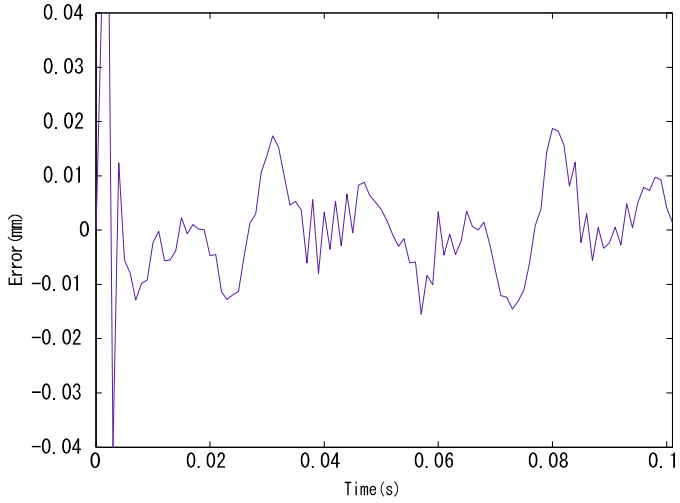

Figure 3.36 RBFNN modeling error with 20[Hz] driving signal

3.3 Comparison of Bouc-Wen model and RBFNN model for Hysteresis Modeling

The Bouc-Wen model and the RBFNN model based on soft computing for hysteresis modeling of piezo electric actuator are already introduced in this chapter. Because the controller for compensation of hysteresis of piezo electric actuator is designed based on hysteresis model which has been already tested, in order to apply precise hysteresis modeling for control design of piezo electric actuator, the best choice of proposed models with different methods need to be selected.

The comparison of the results of Bouc-Wen model and RBFNN model by all the three different algorithms are given in this part so as to choose a precise modeling method for the following research of compensation of hysteresis of piezo electric actuator. The introduction and setting of all the three algorithms has already described in the previous part.

Figure 3.37 shows how Bouc-Wen model optimized with GA, PSO and MSGA proceeds. The three methods for Bouc-Wen hysteresis modeling are tested in the same initial condition, in which the population is 200, and the number of iteration is 150.

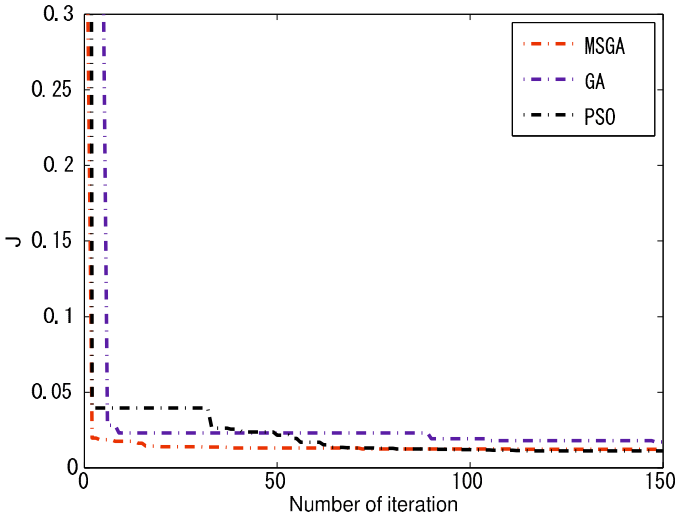

Figure 3.37 Changes of value of J of Bouc-Wen hysteresis modeling for 150 iterations

Figure 3.38 shows how RBFNN model optimized with GA, PSO and

MSGA proceeds. The three methods for RBFNN hysteresis modeling are also tested in the same initial condition, in which the population is 200, and the number of iteration is 150.

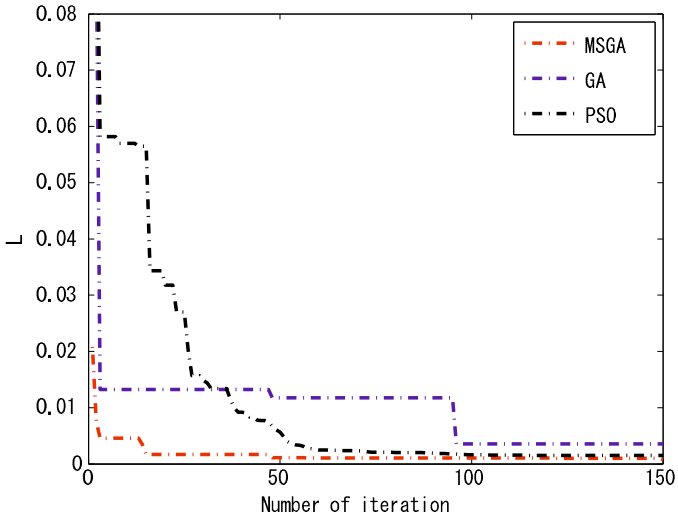

Figure 3.38 Changes of value of J for RBFNN hysteresis modeling 150 iterations

From the results of proceeding of this two models after 150 iterations, it can be found that either for the Bouc-Wen model or for the RBFNN model, MSGA provides both faster convergence than GA and PSO. Furthermore, both fitting results of MSGA and PSO are better than GA.

Table 3.4 RMS error

	Bouc-Wen model			RBFNN model		
	MSGA	GA	PSO	MSGA	GA	PSO
1[Hz]	0.0066	0.0145	0.0123	0.0033	0.0038	0.0019
28[Hz]	0.0543	0.0974	0.0565	0.0208	0.0237	0.0179

In order to demonstrate the performance of hysteresis modeling, experimental verification of the proposed models are shown in Figs.3.39 to 3.46. The RMSE of Bouc-Wen model and RBFNN model is summarized in Table 3.4. First, compared with the results of Bouc-Wen model and RBFNN

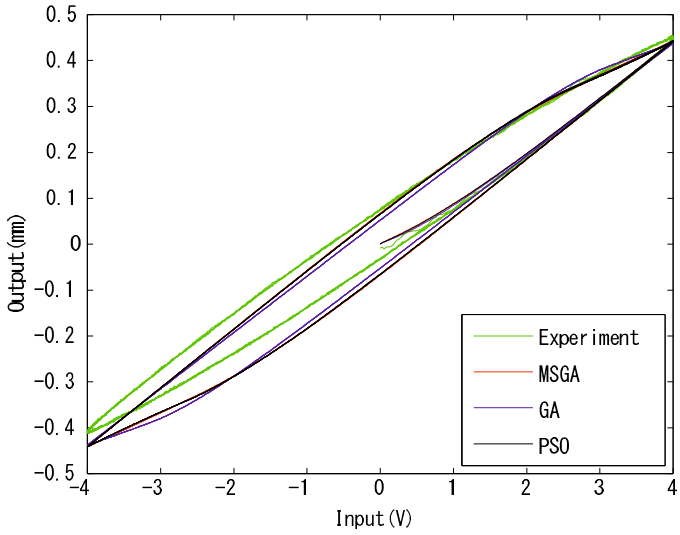

Figure 3.39 Hysteresis performance of Bouc-Wen model under 1[Hz]

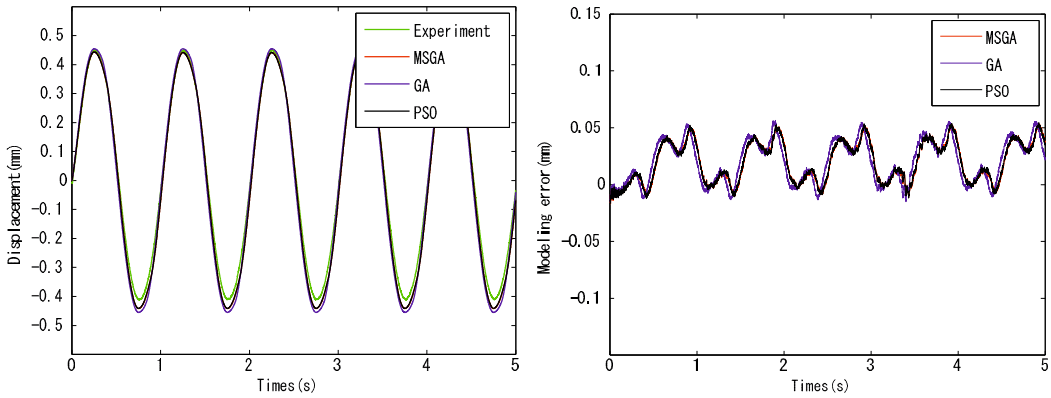

(a) $y(k)$ and $y_m(k)$ (b) Modeling error

Figure 3.40 The output displacement of sinusoidal input excitation of Bouc-Wen model under 1[Hz]

model, it can be seen clearly that although using parameter fitting methods for Bou-Wen model of hysteresis modeling, all the results of RBFNN model are better than Bouc-Wen model. So it's better to apply the more precise RBFNN hysteresis modeling for control design of piezo electric actuator. Then, compared with RBFNN hysteresis modeling based MSGA, GA and PSO, the results have little difference, which shows all the three for RBFNN model can be applied for hysteresis modeling of piezo electric actuator.

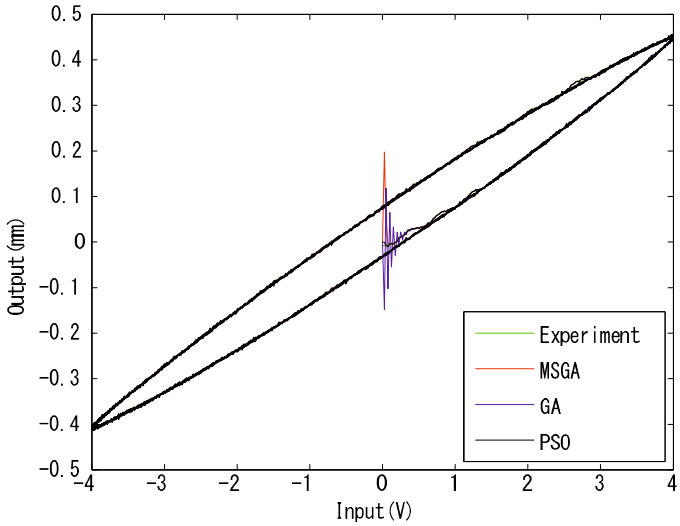

Figure 3.41 Hysteresis performance under of RBFNN model 1[Hz]

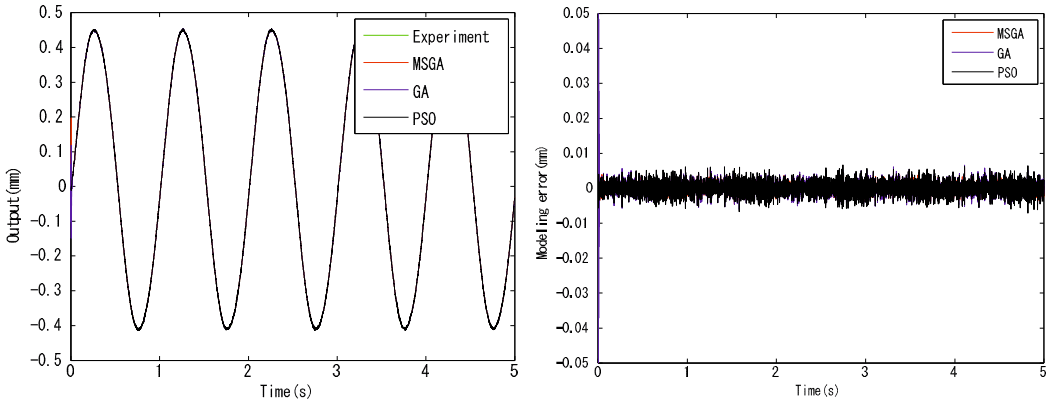

(a) $y(k)$ and $y_m(k)$ (b) Modeling error

Figure 3.42 The output displacement of sinusoidal input excitation of RBFNN model under 1[Hz]

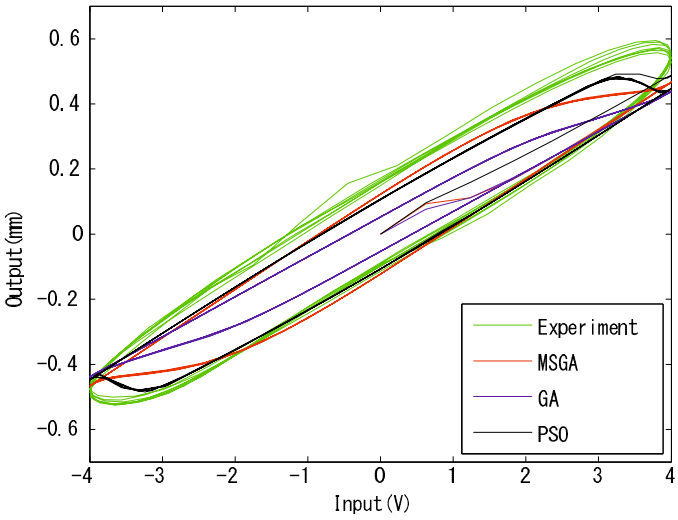

Figure 3.43 Hysteresis performance of Bouc-Wen model under 28[Hz]

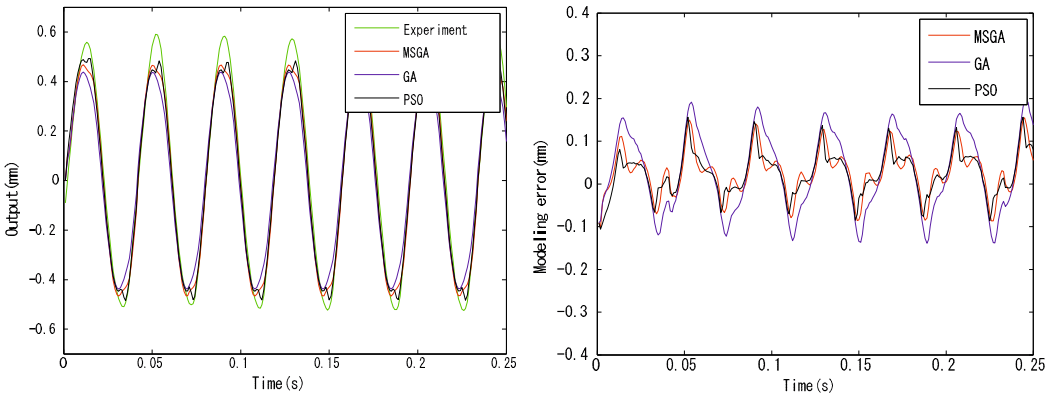

(a) $y(k)$ and $y_m(k)$ (b) Modeling error

Figure 3.44 The output displacement of sinusoidal input excitation of Bouc-Wen model under 28[Hz]

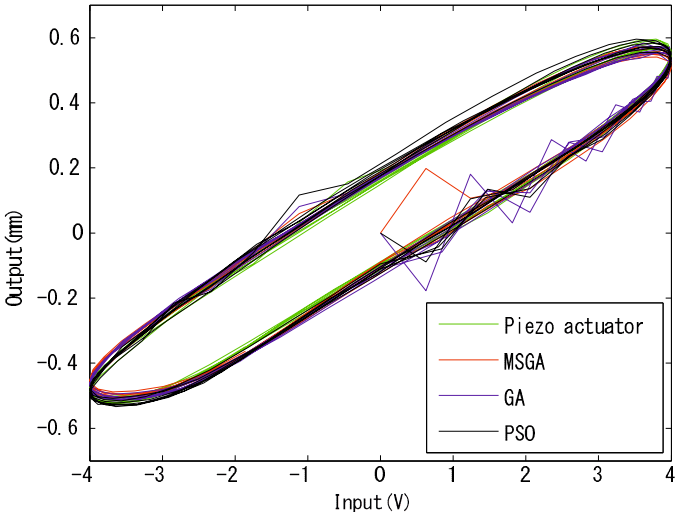

Figure 3.45 Hysteresis performance of RBFNN model under 28[Hz]

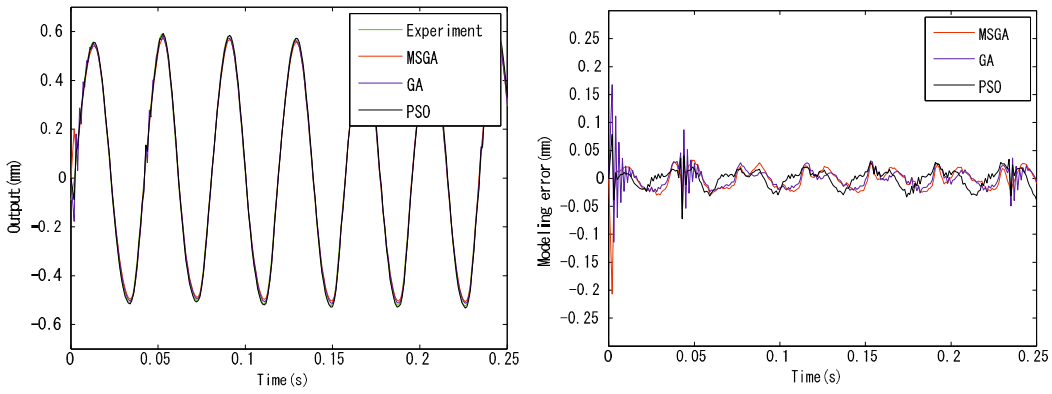

(a) $y(k)$ and $y_m(k)$ (b) Modeling error

Figure 3.46 The output displacement of sinusoidal input excitation of RBFNN model under 28[Hz]

Chapter 4

Compensation of Rate-dependent Hysteresis of Piezo Electric Actuator

4.1 Internal Model Controller Design for Hysteresis Compensation of the Piezo Electric Actuator

This chapter explains the control system design of a positioning control of a piezo electric actuator.

The concept of internal model control (IMC) is treated thoroughly by Morari and Zafiriou in 1989[79]. Figure 4.1 depicts the block digram of principle of classical IMC system, where G_p represents the actual plant, G_m is the model of plant, and G_c is the controller of IMC system.

In the control design of IMC system, if the model is perfect and no disturbances are acting on the system, the feedback signal will be zero. Therefore, the model of plant used for IMC design is very important, the controller of IMC system design requires an accurate model of the plant to be controlled.

With the help of comparison in chapter 3, the results of RBFNN model

performs much better, an adaptive IMC with double RBFNNs is designed for compensation of rate-dependent hysteresis of the piezo electric actuator. In the IMC design, one RBFNN based on PSO is used for hysteresis modeling of piezo electric actuator, while the other RBFNN is given the role of the controller of the IMC system. Figure 4.2 shows the structure of the proposed control system.

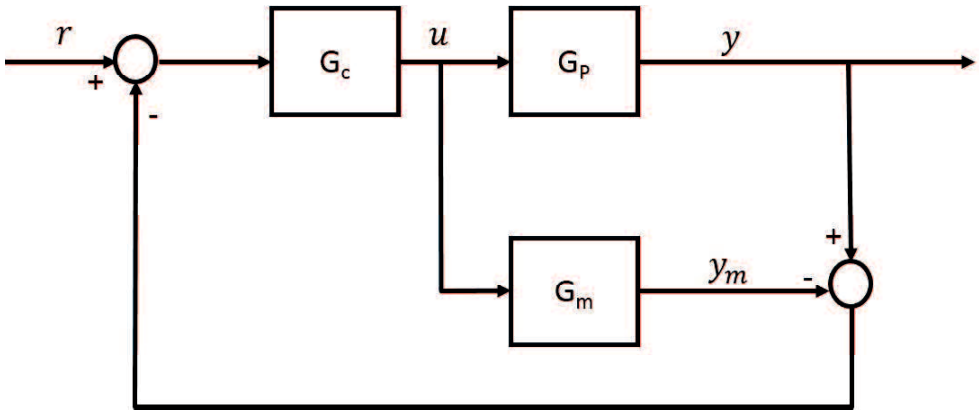

Figure 4.1 Block diagram of classical IMC system

In the process of IMC design, a RBFNN model trained with PSO has been incorporated as the internal model. IMC is suitable for control of a stable plant. It provides good control performance if the model to be embedded in the control system is sufficiently accurate like the case in this study.

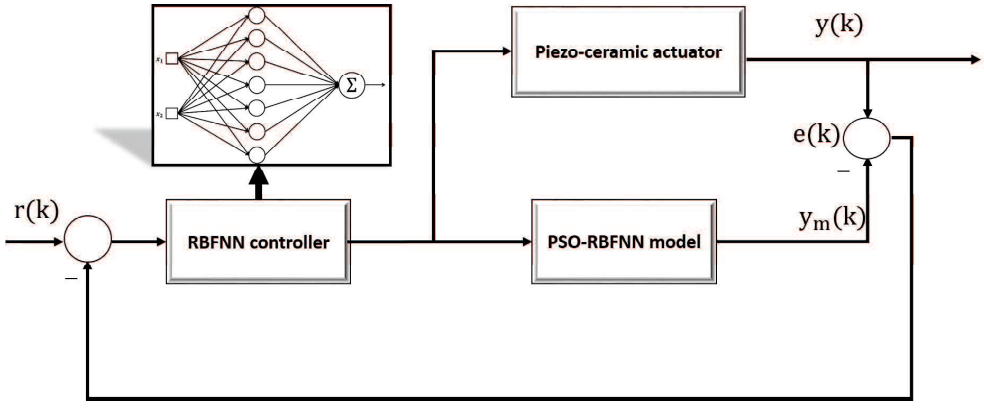

Figure 4.2 Block diagram of control system design

However, due to the rate/frequency-dependent nature of the hysteresis, embedded model might lose accuracy when driving signal frequency and/or speed is altered. This chapter proposes the use of additional RBF neural

network as the controller of the actuator which is adaptively tuned on-line to cope with the possible changes in actuator hysteresis and dynamics as well as to suppress disturbances, as depicted in Fig.4.2. Controller RBFNN is configured to have 2-7-1 structure whose input layer receives the tracking error

$$z_1 = e(k) = y_d(k) - y(k) \tag{4.1}$$

and the rate of error change

$$z_2 = e_c(k) = e(k) - e(k-1), \tag{4.2}$$

where $y_d(k)$ represents the reference position of the actuator at time k. The reason for the choice is that z_1 is used for the tracking control of our piezo actuator, and z_2 is used to suppress jerky response.

Let $\boldsymbol{z} = [z_1, z_2]^T$ be an input signal vector for controller RBFNN. Then output of the activation function of the j-th node of the hidden layer is determined by

$$h_j(k) = \exp\left(\frac{-\|\boldsymbol{z} - \boldsymbol{d}_j\|^2}{2c_j^2}\right) \quad (j = 1, 2, \cdots, 7), \tag{4.3}$$

where $\boldsymbol{d}_j$ and c_j $(j = 1, 2, \cdots, 7)$ correspond to the center and width of radial basis function, respectively. The control input will be synthesized finally by the following equation

$$u(k) = \sum_{j=1}^{7} v_j h_j(k), \tag{4.4}$$

where v_j is the weight for h_j.

The controller is trained to make the tracking error $e(k)$ converge to zero. It is equivalent to learn the inverse rate-dependent hysteresis property of the piezo actuator if there is no modeling error, disturbance and/or measurement noise. The controller should also compensate modeling inaccuracies and disturbances when they are present. In order to increase the efficiency of control process, the conventional back propagation training is employed for the possible need of on-line tuning of the controller parameters, because of its light computational load and convergence speed. Let the target function for controller training be defined by

$$g_c = \frac{(y_d - y)^2}{2} = \frac{e^2}{2}. \tag{4.5}$$

All network parameters $\boldsymbol{d}_j$ and c_j are updated according to its gradient of the tracking error function g_c. The update laws for these parameters are given by the following three equations

$$d_j(k) = d_j(k-1) - \eta \frac{\partial g_c}{\partial d_j} + \beta(d_j(k-1) - d_j(k-2)), \tag{4.6}$$

$$c_j(k) = c_j(k-1) - \eta \frac{\partial g_c}{\partial c_j} + \beta(c_j(k-1) - c_j(k-2)) \tag{4.7}$$

and

$$w_j(k) = w_j(k-1) - \eta \frac{\partial g_c}{\partial w_j} + \beta(w_j(k-1) - w_j(k-2)). \tag{4.8}$$

The parameter $\eta > 0$ in these equations governs the learning rate. The terms starting with β in Eqs.(4.6) (4.7) and (4.8) represent the inertial terms which accelerate learning.

4.2 Results of control experiment

4.2.1 Experimental results at low frequency reference

In the proposed IMC strategy for our piezo electric actuator, the RBFNN controller is used for IMC design. In order to clarify of the proposed control system, a comparison with the proposed RBFNN controller for IMC is necessary.

Another PID controller instead of RBFNN controller for IMC system is applied as a comparison. In addition, because compared with traditional PID controller, the incremental PID controller which is an improvement of PID not only can realize the output of incremental PID easily which is only relevant with last three samplings but also has the effectiveness for initialization[80], if the proposed RBFNN controller for IMC is better than incremental PID, it is also better than the traditional one. So a incremental PID controller is used to validate the performance of proposed RBFNN controller for piezo electric actuator

The incremental form of PID controller is defined by

$$du(k) = k_p[e(k) - e(k-1)] + k_i e(k) + k_d[e(k) - 2e(k-1) + e(k-2)] \quad (4.9)$$

where $e(k)$ is the instantaneous tracking error at time k and $du(k)$ represents the increment of control.

Gains included in this PID control law are set to $(k_p, k_i, k_d) = (1.0, 0.8, 0.6)$ by trial and error.

A feedback positioning control has been performed for a sinusoidal reference input whose frequency changes as a function of time from 1[Hz] to 2[Hz].

The comparison between this two is shown in Fig.4.3 and 4.4 which illustrates the results.

From the results in Fig.4.3, the RMS error based on PID is 0.0259[mm], and the RMS error based on RBFNN is 0.0023[mm], it can be found that the tracking error of PID controller is much lager than RBFNN controller, the propose RBFNN controller delivers excellent tracking for IMC system

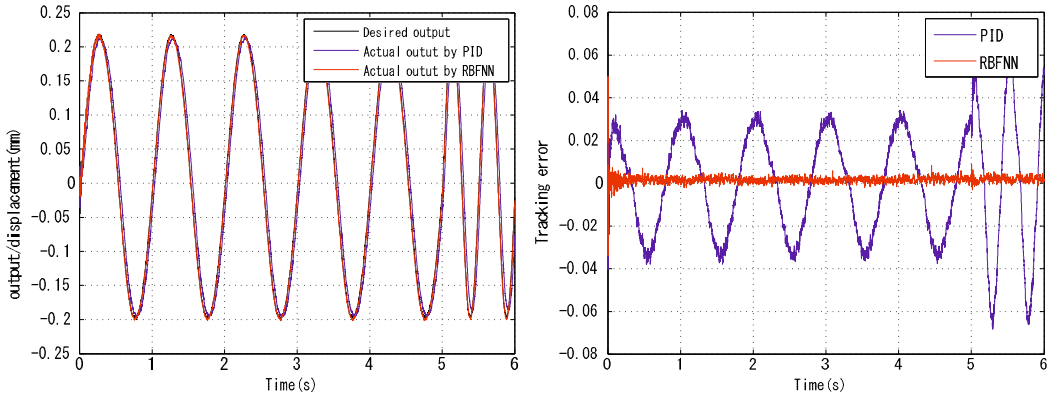

(a) Output displacement (b) Tracking error

Figure 4.3 Results of positioning control simulation for time-varying (1-2[Hz]) frequency reference signal. It is apparent proposed RBFNN-IMC controller outperforms conventional PID controller.

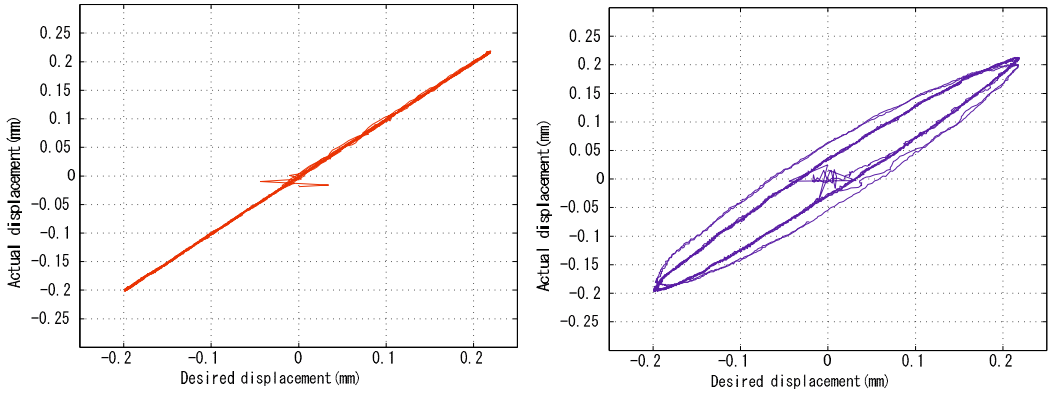

(a) Hysteresis compensation achieved by proposed controller

(b) Hysteresis compensation fails with incremental PID controller

Figure 4.4 Difference of hysteresis compensation performance: (a)Proposed controller and (b)Conventional PID

design while incremental PID results in a poor performance. The trajectory in Fig.4.3 also shows the incremental PID controller fails to compensate the hysteresis of piezo electric actuator as well.

4.2.2 Experimental results at middle frequency reference

The control results at low frequency have been already given above. Furthermore, in order to observe the performance of proposed double RBFNNs adaptive IMC control system, two sinusoidal positioning command signals at middle frequency are given as the reference of the adaptive positioning control system experiment, while the frequency varies with time: to be specific, 1-3[Hz] and 1-4[Hz] respectively.

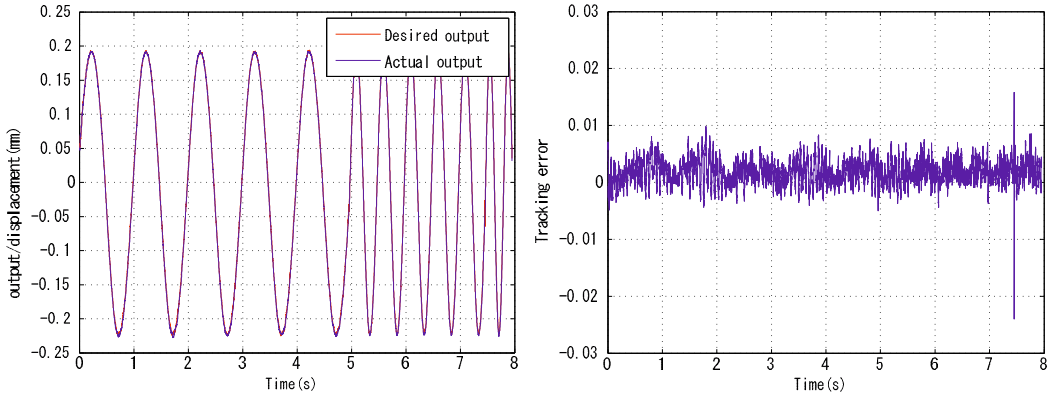

(a) Output displacement (b) Tracking error

Figure 4.5 Adaptive control experimental results of 1-3[Hz] input

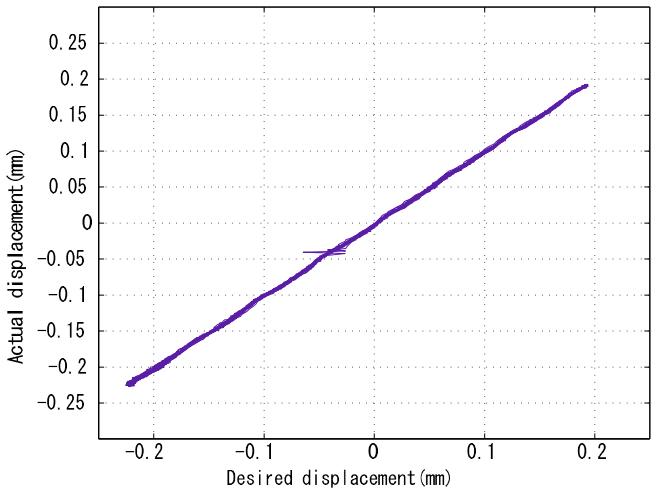

Figure 4.6 Hysteresis compensation performance when 1-3[Hz] time varying frequency reference signal is given to the system

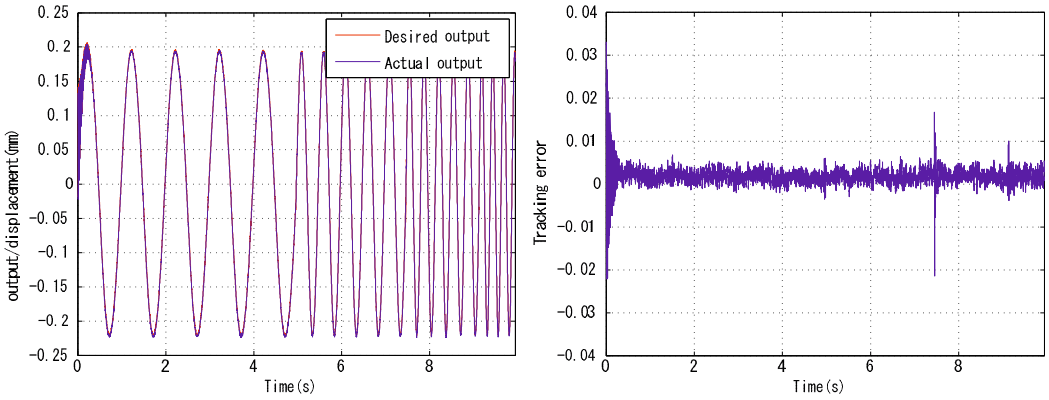

(a) Output displacement (b) Tracking error

Figure 4.7 Adaptive control experimental results of 1-4[Hz] input

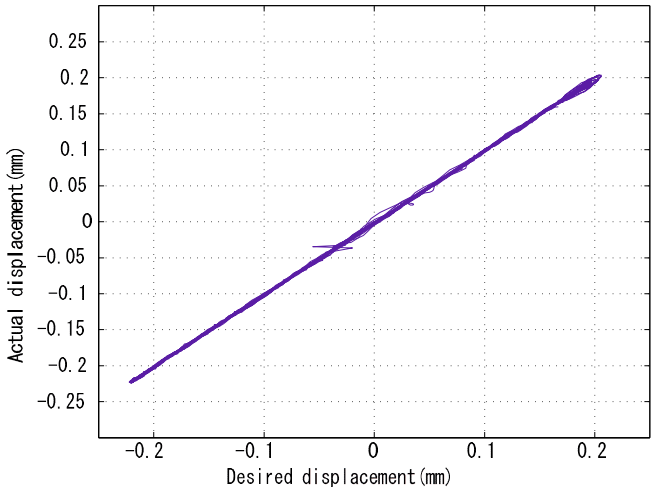

Figure 4.8 Hysteresis compensation performance when 1-4[Hz] time varying frequency reference signal is given to the system

Figs.4.5 and 4.7 separately give the tracking control performance for 2 different reference signals at middle frequency in time domain, whereas Figs.4.6 and 4.8 show the results of hysteresis compensation performance. The RMS error at 1-3[Hz] is 0.0028[mm] and the RMS error at 1-4[Hz] is 0.0031[mm], the results show the proposed adaptive internal model control system with double RBFNNs performs quite well at middle frequency for compensation of rate-dependent hysteresis of our piezo electric actuator.

4.2.3 Experimental results at high frequency reference

Finally, another control experimental results of proposed double RBFNNs adaptive IMC control system for sinusoidal reference input at high frequency whose frequency changes as a function of time from 1 to 10[Hz] is also shown in this part.

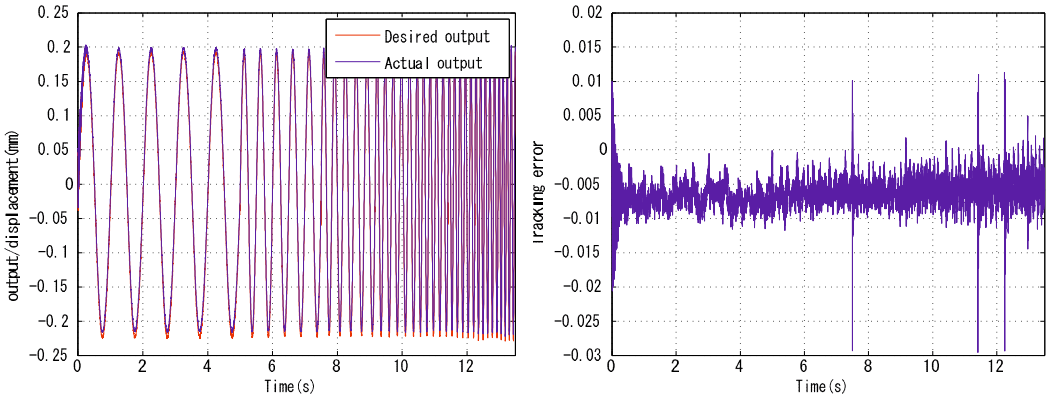

(a) Output displacement (b) Tracking error

Figure 4.9 Adaptive control experimental results of 1-10[Hz] input

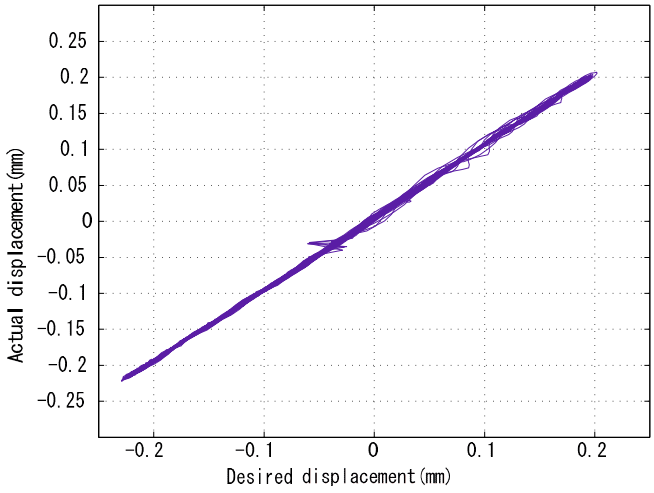

Figure 4.10 Hysteresis compensation performance when 1-10[Hz] time varying frequency reference signal is given to the system

The output displacement and tracking error of proposed control scheme are separately shown in Fig.4.9(a) and 4.9(b), whereas Fig.4.10 shows the hysteresis compensation performance.

Table 4.1 RMS error at different frequencies

	1-3[Hz]	1-4[Hz]	1-10[Hz]
RMSE	0.0028[mm]	0.0031[mm]	0.0067[mm]

Table 4.1 summarizes the RMS error of the experiments above. It can be found the proposed adaptive internal model control system with double RBFNNs also perform well at high frequency of our piezo electric actuator, but the tracking error will increase as the frequency of input increases, the response tends to be oscillatory as input frequency increases. This might be caused by discontinuous change of the frequency of the reference and resonance of the actuator. Such a low frequency resonance might occur because the bimorph actuator is thin in its shape.

The transient part of the responses have been removed from the plots for the latter three figures in order to illustrate that proposed controller maintains hysteresis compensation performance even when driving frequency is altered. Transient tracking performance can be seen in the former three figures in the time domain. Relatively large tracking errors are observed in Figs.4.7 and 4.9 at the beginning of control. But it can also be seen in these figures that real time BP controller tuning works and the errors have been attenuated significantly within a single second.

Chapter 5

Conclusion

5.1 Summary and Contribution

This dissertation discloses the results of researches focusing on the application of RBF neural networks and bio inspired algorithms for modeling and compensation of rate-dependent hysteresis of a piezo electric actuator. The proposed methods, analysis and results of experiments have been summarized as follows.

Firstly, the research on Bouc-Wen model with MSGA for piezo electric actuator is summarized in this part. MSGA has flexible structure and better performance on convergence time and precision, it is employed for parameter identification of Bouc-Wen model in an efficient way. MSGA is so flexible that there is also a room for improvement to acquire accurate model. In order to verify the performance of the method in a comparative manner, classical GA ans PSO are also applied for Bouc-Wen model. The displacement output results of Bouc-Wen model show that the modeling error will increase under different frequencies, but the Bouc-Wen model identified with MSGA can capture the hysteresis for our piezo electric actuator and performed better than GA based model. Results of modeling error often remains at the maximum and minimum of model output. It may result from the structural error of the Bouc-Wen model used for the piezo electric actuator.

Then an RBF neural network is designed as a hysteretic model to char-

acterize rate-dependent hysteresis of piezo electric actuator. In order to increase precision of the adaptive RBFNN modeling, PSO algorithm is applied to optimize the parameters of the RBF neural network model, and number of the iteration is found to be another factor for our modeling, and adjusting the number of iterations is done to get better performance. The results of hysteresis modeling illustrate that this proposed RBFNN model trained with PSO performed very well. The RBFNN hysteresis modeling based on MSGA and GA has also been tested in this research.

The comparison between Bouc-Wen model and RBFNN model shows the results of RBFNN hysteresis modeling performs better and more efficient than Bouc-Wen hysteresis modeling, MSGA provides both faster convergence than GA and PSO, both fitting results of MSGA and PSO are better than GA, and limitations happened in the Bouc-Wen model can be solved by RBFNN model. So the RBFNN model based on PSO is applied for the following research of control design for compensation of rate-dependent hysteresis of our piezo electric actuator.

An adaptive double RBF neural networks internal model control system for piezo electric actuator has been presented in the dissertation. Two RBFNNs are used in the proposed control system, one RBFNN trained with PSO serves as the internal model of the actuator with rate-dependent hysteresis, whereas the other RBFNN based on PSO is configured as the IMC controller which is tuned on-line by the classical back propagation algorithm with inertia term.

Results of the experiment indicate that proposed control system can compensate the hysteresis under several different reference signals for our piezo electric actuator. However, the response tends to be oscillatory as input frequency increases. This might be caused by discontinuous change of the frequency of the reference and resonance of the actuator. Such a low frequency resonance might occur because the bimorph actuator is thin in its shape.

5.2 Future work

Based on the results obtained in this research, there still remains many problems and works which should be solved and improved.

More works need to be done for the compensator design for variety of different piezo electric actuators which covers wide range of operating conditions. As mentioned in the research of Bouc-Wen model, problems of the maximum and minimum modeling error should be improved. The bio inspired algorithms like flexible MSGA still should be designed more suitable for on line control application, improvement of MSGA should be sought for online control system design. Along with the high-precision systems, the research works should continue to achieve the control design for systems with ultra high frequencies.

Reference

[1] J.L. Fanson and T.K. Caigjey, Positive position feedback control for large space structures, Amer.Ins.aeronaut.Astronaut.J., vol. 28, pp. 717-724, 1990.

[2] O. Gomis-Bellmunt, F. Ikhouane and D. Montesinos-Miracle, Control of a Piezo Electric Actuator Considering Hysteresis, Journal of Sound and Vibration, pp. 383-399, 1990.

[3] P. Mahyan, K. Srinivasan, S. Watechagit and G. Washington, Dynamic Modeling and Controller Design for a Piezoelectric Actuation System Used for Machine Tool Control, J. Intell. Mater. Syst. Struct., vol. 11, pp. 771-780, 2000.

[4] S. Majima, K. dodama and T. Hasegawa, Modeling of Shape Memory Alloy Actuator and Tracking Control System with the Model, IEEE Trans. Control syst. Technol., vol. 9, No 1, pp. 54-59, 2001.

[5] M. Goldfarb and N. Celanovic, Modeling piezoelectric stack actuators for control of micromanipulation, IEEEConr.Syst.Mag., vol. 17, no.3, pp. 69-79, 1997.

[6] Ralph C. Smith, Smart Material System: Model Development, Society of Industrial and Applied Mathematics, Raleigh. North Carolina, 2005.

[7] J.C. Bruch Jr, J.M. Sloss, S. Adali, and I.S Sadek, "Optimal piezoactuator locations/lengths and applied voltage for shape control of beam," Smart Mater. Struct., vol. 19, pp. 205-211, 2000.

[8] JL. Ha, RF. Fung and CS. Yang, Hysteresis Identification and Dynamic Responses of the Impact Drive mechanism. J Sound Vib, vol. 283, pp. 943-956, 2005.

[9] Preisach F., Uber die magnetische Nachwirkung, Zeitschrift fur Physik, vol. 94, pp. 277-302, 1935.

[10] Mayergoyz and D. Isaak, Mathematical Models of Hystersis, IEEE transactions on magnetics, vol. Mag-22, NO. 5, 1986.

[11] J.K. Park, G. Washington, Prediction of hysteretic effects in PZT stack actuators using a hybrid modeling strategy, J.Smart Struct. Mater. :Model., Signal Process., Control 5383, pp.48-59, 2004.

[12] G. Song, J.Q. Zhao and X.Q. Zhou, J.A. de Abreu-Garcia, Tracking control of a piezo ceramic actuator with hysteresis compensation using inverse Preisach model, IEEE/ASME Trans. Mechatron. vol 10, pp.198-209, 2005.

[13] F. Schreiber, Y. Sklyarenko, K. Schluter and J.Schmitt, Tracking control with hysteresis compensation for manipulator segments driven by pneumatic artificial muscles, Proceedings of IEEE International Conference on Robotics and Biomimetics, pp.2750-2755, 2011.

[14] L. Zhi, C.Y. Su and C. Tianyou, Compensation of hysteresis nonlinearity in magnetostrictive actuators with inverse multiplicative structure for Preisach model, IEEE Trans. Autom. Sci. Eng., pp.1-7, 2013.

[15] A .Bahar, F. Pozo, L. Acho and J. Rodellar, A. Barbat, Parameter identification of large-scale magnetorheological dampers in a benchmark building, J. Comput. Struct., vol 88, pp.198-206, 2010.

[16] W. Zhenyan, Z. Zhen, M. Jianqin and Z. Kemin, A Hammerstein-based model for rate-dependent hysteresis in piezoelectric actuator, Proceedings of the 24th Chinese Control and Decision Conference, pp.1391-1396, 2012.

[17] Qingsong Xu, Identification and compensation of piezo electric hysteresis without modeling hysteresis inverse, IEEE Trans. Ind. Electron., vol 60, pp.3927-3937, 2013.

[18] G.R. Yu, L.W. Haung, Optimal control of a nano-positioning stage using linear matrix inequality and hierarchical genetic algorithms, Proceedings of IEEE International Conference on Systems, Man and Cybernetics, pp.2833-2838, 2008.

[19] Xin Kai Li, Yingshe Luo, Yuanwei Qi and Rong Zhang, On non-Newtonian lubrication with the upper convected Maxwell model, Applied Mathematical Modelling, vol 35, pp.2309-2323, 2011.

[20] M. Quant, H. Elizalde, A. Flores, R. Ramirez, P. Orta, G.B. Song, A comprehensive model for piezoceramic actuators: modelling, validation and application, J. Smart Mater. Struct. 18(12), 2009.

[21] N. Miri, M. Mohammadzaheri, L. Chen, A comparative study of different physics-based approaches to modeling of piezoelectric actuators, Proceedings of IEEE/ASME International Conference on Advanced Intellignet Mechatronics(AIM), pp.1211-1216, 2013.

[22] T. Tjahjowidodo, F. Al-Bender, H. Van Brussel, W. Symens, Friction characterization and compensation in electro-mechanical systems, Int.J.Sound Vib., pp.632-646, 2007.

[23] Ying Feng, Camille Alain Rabbath, Tianyou Chai, C.Y. Su, Robust adaptive control of systems with hysteretic nonlinearities: a duhem hysteresis modeling approach, Proceedings of IEEE AFRICON, 2009.

[24] Juan Du, Ying Feng, C.Y. Su, Y.M. Hu, On robust control of systems preceded by Coleman-Hodgdon hysteresis, Proceedings of IEEE International Conference on Control and Automation, pp.685-689, 2009.

[25] Kwangsoo Ho, A thermodynamically consistent model for magnetic hysteresis, Journal of Magnetism and Magnetic Materials, vol 357, pp.93-96, 2014.

[26] Y.Q. Ni, Z.G. Ying, J.M. Ko, W.Q. Zhu, Random response of integrable Duhem hysteretic systems under non-white excitation, International Journal of Non-Linear Mechanics, vol 37, pp.1407-1419, 2002.

[27] G.Y. Gu, L.M. Zhu, C.Y. Su, Modeling and compensation of a symmetric hysteresis nonlinearity for piezoceramic actuators with a modified Prandtl-Ishlinskii model, IEEE Trans. Ind. Electron., vol 61, pp.1583-1595, 2013.

[28] S. Bashash, N. Jalili, A polynomial-based linear mapping strategy for feedforward compensation of hysteresis in piezo electric actuators, Trans. ASME J. Dyn. Sys., Meas. Control, vol 130, 2008.

[29] P.Liu, Z. Zhang, J. Mao, Modeling and control for giant magnetostrictive actuators with rate-dependent hysteresis, J. Appl. Math. 2013, pp.1-8, 2013.

[30] Qingsong Xu, Pak-Kin Wong, Hysteresis modeling and compensation of a piezostage using least squares support vector machines, Mechatronics, vol 21, pp.1239-1251, 2011.

[31] T.N. Do, T. Tjahjowidodo, M.W.S. Lau, S.J. Phee, An investigation of friction-based tendons heath model appropriate for control purposes, Mech. Syst. Signal Process., vol 42, pp.97-114, 2013.

[32] D.Y. Abramovitch, S. Hoen, R. Workman, Semi-automatic tuning of PID gains for atomic force micro scopes, Asian J. Control, vol 11, pp.188-195, 2009.

[33] T.H. Nguyen, N.M. Kwok, Q.P. Ha, J. Li and B. Samali, Adaptive sliding mode control for civil structures using magnetorheological dampers, Proceedings of International Symposium on Automation and Robotics in Constructions, pp.636-641, 2006.

[34] C.Y.Su, Y. Stepanenko, J. Svoboda, T.P. Leung, Robust adaptive control of a class of nonlinear systems with unknown backlash-like hysteresis, IEEE Trans. Autom. Control, vol 45, pp.2427-2432, 2000.

[35] A. Esbrook, T. Xiaobo, H.K. Khalil, Control of systems with hysteresis via servo compensation and its application to nanopositioning, IEEE Trans. Control Syst. Technol., vol 21, pp.725-738, 2013.

[36] L. Yangmin, X. Qingsong, Adaptive sliding mode control with perturbation estimation and PID sliding surface for motion tracking of a piezo-driven micro manipulator, IEEE Trans. Control Syst. Technol., vol 18, pp.798-810, 2010.

[37] Y. Yu, Z. Xiao, NG Naganathan, RV Dukkipati, Dynamic Preisach Modelling of Hysteresis for the Piezoceramic Actuator System, Mechanism and Machine Theory, vol. 37, pp. 75-89, 2002.

[38] Y. Ueda, F. Fujii and D. Liu, Identification of hysteresis using adaptive Preisach model, The Japan Society of Mechanical Engineers, vol 81, No. 830, 2015.

[39] Bouc and R., Forced Vibration of Mechanical Systems with Hysteresis, Proceedings of the Fourth Conference on Nonlinear Oscillation, 1967.

[40] Wen and Y. K., Method for Random Vibration of Hysteretic Systems, Journal of Engineering Mechanics, vol. 102(2), pp. 249-263, 1976.

[41] A. Dominguez, R. Sedaghati and I. Stiharu, Modeling and Application of MR Dampers in Semi-adaptive Structures, Comput Struct, vol. 86, pp. 407-415, 2008.

[42] X. Lu, Q. Zhou, Dynamic Analysis Method of A Combined Energy Dissipation System and Its Experimental Verification, Earthquake Eng Struct Dyn, vol. 31, pp. 1251-1265, 2002.

[43] J. Song, A. Der Kiureghian, JL. Sackman, Seismic Interaction in Electrical Substation Equipment Connected by Non-linear Rigid Bus Conductors. Earthquake Eng Struct Dyn, vol. 36, pp. 167-190, 2007.

[44] J. Lee, D. Lee, S. Won, Precise tracking control of Piezo actuator using sliding model control with feedforward compensation, SICE Annual Conference 2010, pp. 1244-1249, 2010.

[45] T.J. Yeh, S.W. Lu, T.Y. Yu, Modeling and identification of hysteresis in piezoelectric actuators, J. Dyn. Syst, Meas. Control-Trans. ASME 128, pp. 189-196, 2006.

[46] Vo-Minh. Tri, T. Tjahjowidodo, H. Ramon, H. Van Brussel, A new approach to modeling hysteresis in a pneumatic artificial muscle, IEEE/ASME Trans. Mechatron., vol 16, pp. 177-186, 2011.

[47] X.S. Wang, X.J. Wang, Y. Mao, Hysteresis compensation in GMA actuators using Duhem model, Proceeding of the 7th World Congress on intelligent Control and Automation, pp. 388-393, 2008.

[48] S. Rosenbaum, M. Ruderman, T. Strohla, T. Bertram, Use of Jiles-Atherton and Piesach hysteresis models for inverse feed-forward control, IEEE Trans. Magn. 46, pp. 3984-3989, 2008.

[49] M.Al. Janaideh, P. Krejci, Inverse rate-dependent Prandtl-Ishlinskii model for feedforward compensation of hysteresis in a piezo micro positioning actuator, IEEE/ASME Trans. Mechatron. vol 18, pp. 1498-1507, 2012.

[50] M. Rakotondrabe, Bouc-Wen modeling and inverse multiplicative structure to compensation hysteresis nonlinearity in piezoelectric actuators, IEEE Trans. Automation Science and Engineering 8, pp. 428-431, 2011.

[51] Hsin-Jang Shieh , Yun-Jen Chiu , Yen-Ting Chen , Optimal PID control system of a piezoelectric microospitioner, Proceeding of 2008 IEEE/SICE international Symposium on System Integration, pp. 1-5, 2008.

[52] K.C. Lu, C.H. Loh, J.N. Yang, P.Y. Lin, Decentralized sliding model control of a building using MR dampers, Smart Mater. Struct., vol 17, pp. 1-5, 2008.

[53] Chi-Ying Lin , Neural Network Adaptive Control and Repetitive Control for High Performance Precision Motion Control, SICE Annual conference 2010, pp. 2843-2844, 2010.

[54] Y. Okazaki, A micro-positioning tool post using a piezoelectric actuator for diamond turning machines, Precis. Eng, vol. 12, (1990), pp. 151-156.

[55] Koichi Hata, Md Nazir Muhamed and Fumitake Fujii, Study on RateDependent Hysteresis Compensation of Piezo-Ceramic Actuator, International Journal of Engineering Innovation and Management 2, 2012.

[56] D.W. Song, C.J. Li, Modeling of piezo actuator's nonlinear and frequency dependent dynamics, J. Mechatron, pp. 391-410, 1999.

[57] A. Raghavan, P. Seshu, P.S. Gandhi, Hysteresis modelling in piezo ceramic actuator systems, S. Mohan, B. Dattaguru, S. Gopalakrishnan (Eds.), Journal of Smar Materials, Structures and System, vol. 5062, pp. 560-567, 2003.

[58] Z. Szabo, I. Tugyi, G. Kadar, J. Fuzi, Identification procedures for scalar Preisach model, J.Phys.B: Condens. Matter, 343, pp. 142-147, 2004.

[59] K.K. Ahn, B.K. Nguyen, Optimal proportional-integral-derivative control of shape memory alloy actuators using genetic algorithm and the Preisach model, Proc. Inst. Mecha. Eng. PartI-J. Syst. Control Eng, 221, pp.531-540, 2007.

[60] G.R. Yu, C.S. You, R.J. Hong, Self-tuning fuzzy control of a piezo electric actuator system, Proceedings of the IEEE International Conference on Systems, Man and Cybernetics, vols.1-6, pp.1108-1113, 2006.

[61] A.F. Payam, M. Fathipour, M.J. Yazdanpanah, A back stepping controller for piezo electric actuators with hysteresis in nano positioning, Proceedings of the IEEE International Conference on Nano/Micro-Engineered and Molecular Systems, pp.711-716, 2009.

[62] S. Kagami, ART-Linux for High-frequency System, Proceeding of 2013 IEEE 1st International Conference on Cyber-Physical Systems, Networks, and Applications (CPSNA), pp. 60-65, 2013.

[63] A. Mielke and T. Roubicek, A Rate-Independent Model for Inelastic Behavior of Shape-Memory Alloys, Multiscale Model. Simul., 1(4), 571-597, 2003

[64] D.S. Broomhead, David Lowe, Radial basis functions, multi-variable functional interpolation and adaptive networks, RSRE-MEMO-4148, 1988.

[65] D.S. Broomhead, David Lowe, Multivariable functional interpolation and adaptive networks, Complex Systems 2, pp.321-355, 1988.

[66] R.Eberhart and J.Kennedy, A new optimizer using particle swarm theory, Proc. 6th IEEE International Symposium on Micro Machine an Human Science(MHS), pp. 39-43, 1995.

[67] Mitchell, Melanie. An Introduction to Genetic Algorithms. Cambridge, MA: MIT Press, 1996.

[68] Gh. Paun, A Quick Introduction to Membrane Computing, The Journal of Logic and Algebraic Programming, vol. 79, pp. 291-294, 2010.

[69] I.I. Ardelean, D. Besozzi: Mechanosensitive Channels, a Hot Topic in (Micro) Biology: Any Excitement for P Systems?, In Brainstorming Week on Membrane Computing, Technical Report No 26/03, 32-36, 2003.

[70] Calude, C. S., and Paun, Bio-steps beyond Turing, Biosystems, vol.77, pp.175-194, 2004.

[71] T.Y. Nishida, An Approximate Algorithm for NP-complete Optimization Problems Exploiting P system, The Brainstorming Workshop on Uncertainty in Membrane Computing, pp185-192, 2004.

[72] A. Leporati, D. Pagani, A membrane Algorithm for the Min storing Problem. Proceedings of Membrane Computing, International Workshop, WMC7, pp.397-416, 2006.

[73] Nishida T.Y., Application of P system: a new algorithm for NP-complete optimization problem. Proceedings of The 8th World Multi-Conference on Systems, Cybernetics and Informatics, pp.109-112, 2004.

[74] Dongbo Liu, Xiucheng Dong and Peng Shi, The optimization based on improved membrane algorithm for fuzzy RBF neural network control of ball-plate system, ICIC Express Letters, Part B: Applications, Vol. 3, pp. 1259-1267, 2012.

[75] Karam M. Elbayomy, Jiao Zongxia, Zhang Huaqing, PID Controller Optimization by GA and Its Performances on the Electro-hydraulic Servo

Control System, Chinese Journal of Aeronautics, vol 21, pp.378-384, 2008.

[76] Zafer Bingul, Oguzhan Karahan, A Fuzzy Logic Controller Tuned with PSO for 2 DOF Robot Trajectory Control, Expert Systems with Applications, vol 38, pp.1017-1031, 2011.

[77] Giuditta Franco, Natasa Jonoskab, Barbara Osborn, and Anna Plaas, Knee joint injury and repair modeled by membrane systems, Expert Systems with Applications, vol 38, pp.1017-1031, 2011.

[78] Daniela Besozzi, Paolo Cazzaniga, Dario Pescini and Giancarlo Mauri, Modeling metapopulations with stochastic membrane system, Biosystems, vol 91, pp.499-514, 2008.

[79] M. Morari and E. Zafirious, Robust Process Control, Prentice-Hall, 1990.

[80] L. Shen, Z. Liu, Z. Zhang and X. Shi, Frame-level bit allocation based on incremental PID algorithm and frame complexity estimation, J. Vis. Commun. Image R., vol 17, , pp. 28-34, 2009.

Acknowledgment

I would like to express my deepest gratitude to my teacher, Professor Fumitake Fujii, in Graduate School of Science and Engineering, Yamaguchi University, for his great suggestions, constant encouragement and guidance on my research. I do appreciate his patience, encouragement and professional instructions during my PHD study and research.

And I also would like to express my heartfelt gratitude to Professor Zhongwei Jiang, Kanya Tanaka, Masanao Obayashi and Kakuji Ogawara in Graduate School of Science and Engineering, Yamaguchi University. According to the useful and kind reviews, comments and advices from them, the thesis become better and better, make the thesis have great improvement.

I also owe my sincere gratitude to all my friends who gave me a lot of help. I should finally thank to my family for the kind and great consideration to me all through the period, who have gave me lots of support.